Trace element and isotope constraints on crustal anatexis by upwelling mantle melts in the North Atlantic Igneous Province: an example from the Isle of Rum, NW Scotland

ROMAIN MEYER*, GRAEME R. NICOLL†, JAN HERTOGEN*‡, VALENTIN R. TROLL†§,
ROBERT M. ELLAM¶ & C. HENRY EMELEUS#

*Geo-Instituut, Katholieke Universiteit Leuven, Celestijnenlaan 200E, B-3001 Leuven-Heverlee, Belgium
†Department of Geology, University of Dublin, Trinity College, Dublin 2, Ireland
§Department of Earth Sciences, Uppsala Universitet, Villavägen 16, SE-752 36 Uppsala, Sweden (present address)
¶Scottish Universities Environmental Research Centre, Rankine Ave., East Kilbride G75 0QF, UK
#Department of Earth Sciences, University of Durham, Durham DH1 3LE, UK

Abstract – Sr and Nd isotope ratios, together with lithophile trace elements, have been measured in a representative set of igneous rocks and Lewisian gneisses from the Isle of Rum in order to unravel the petrogenesis of the felsic rocks that erupted in the early stages of Palaeogene magmatism in the North Atlantic Igneous Province (NAIP). The Rum rhyodacites appear to be the products of large amounts of melting of Lewisian amphibolite gneiss. The Sr and Nd isotopic composition of the magmas can be explained without invoking an additional granulitic crustal component. Concentrations of the trace element Cs in the rhyodacites strongly suggests that the gneiss parent rock had experienced Cs and Rb loss prior to Palaeogene times, possibly during a Caledonian event. This depletion caused heterogeneity with respect to $^{87}Sr/^{86}Sr$ in the crustal source of silicic melts. Other igneous rock types on Rum (dacites, early gabbros) are mixtures of crustal melts and and primary mantle melts. Forward Rare Earth Element modelling shows that late stage picritic melts on Rum are close analogues for the parent melts of the Rum Layered Suite, and for the mantle melts that caused crustal anatexis of the Lewisian gneiss. These primary mantle melts have close affinities to Mid-Oceanic Ridge Basalts (MORB), whose trace element content varies from slightly depleted to slightly enriched. Crustal anatexis is a common process in the rift-to-drift evolution during continental break-up and the formation of Volcanic Rifted Margins systems. The 'early felsic–later mafic' volcanic rock associations from Rum are compared to similar associations recovered from the now-drowned seaward-dipping wedges on the shelf of SE Greenland and on the Vøring Plateau (Norwegian Sea). These three regions show geochemical differences that result from variations in the regional crustal composition and the depth at which crustal anatexis took place.

Keywords: North Atlantic Igneous Province, Isle of Rum, Vøring Margin, Volcanic Rifted Margins, crustal contamination, crustal anatexis, petrogenesis.

1. Introduction

The Eurasian–Greenland continental break-up during the Paleocene–Eocene transition marked the culmination of a continental rift system and the development of Volcanic Rifted Margins (Saunders *et al.* 1997; Meyer, van Wijk & Gernigon, 2007). Up to the end of the Danian stage, the early geodynamic history of this continental break-up is marked by widespread extensional basin formation and localized minor magmatism. A first peak of volcanic activity around 60 Ma caused continental flood basalt eruptions and formed numerous large central volcanoes whose eroded remnants now crop out as igneous centres in West and East Greenland, NE Ireland and NW Scotland (Emeleus & Bell, 2005). A second 'pulse' of high magma eruption rates at *c*. 55 Ma coincided with the final break-up of the continents and the initiation

of seafloor spreading, and emplaced the volcanic seaward-dipping wedges (Saunders *et al.* 1997). The Volcanic Rifted Margins igneous formations of the North Atlantic Igneous Province (NAIP) extend over an area of 1.3×10^6 km^2 and cover nearly the whole length of the conjugate NE Atlantic margins (Saunders *et al.* 1997; Eldholm *et al.* 2000).

Different Volcanic Rifted Margins structural zones characterize distinct time–space episodes of the rift-to-drift evolution history (Fig. 1) (Eldholm *et al.* 2000; Menzies *et al.* 2002; Coffin & Eldholm, 2005): (a) continental flood basalt areas mark the late stage of a continental rift; (b) the seaward-dipping wedges are extrusive rock units from the rift-to-drift transition; (c) High Velocity Lower Crustal bodies presumably reflect massive intrusive complexes near the Continent Ocean Boundary. Unfortunately, even with state-of-the-art drilling techniques, the High Velocity Lower Crustal bodies will remain an unreachable drilling target for the time being. The specific structure of

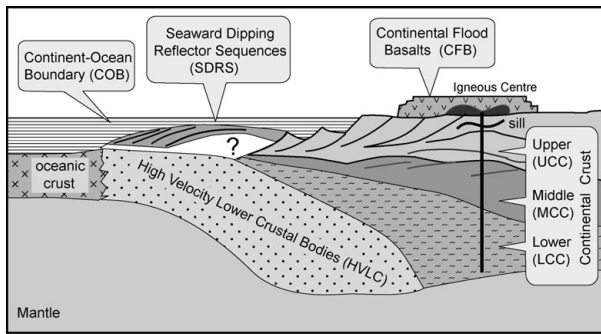‡Author for correspondence: jan.hertogen@geo.kuleuven.be

Figure 1. Schematic tectono-magmatic division of a Volcanic Rifted Margin (VRM) system. VRMs characteristically comprise three zones: Continental Flood Basalt (CFB) areas, Seaward-Dipping Reflector Sequences (SDRS) and High Velocity Lower Crustal bodies (HVLC) next to the Continent Ocean Boundary (COB). UCC, MCC, LCC – Upper, Middle and Lower Continental Crust (modified from Eldholm *et al.* 2000, and Menzies *et al.* 2002).

CLF = Canna Lava Formation, LS = Ultrabasic Layered Suite, NMZ = Northern Marginal Zone
SMZ = Southern Mountains Zone, WG = Western Granite, Mes = Mesozoic sediments,
Tor = Torridon Group Sandstone

Figure 2. Geological sketch map of the Isle of Rum (modified from Emeleus & Bell, 2005).

these tectono-magmatic crustal zones depends on the interaction of lithospheric and asthenospheric properties and dynamics of rifting and magma supply during the formation of a Volcanic Rifted Margins system.

The Paleocene magmatism of the Isle of Rum in NW Scotland forms an integral part of the pre-break-up NAIP continental-flood-basalt tectono-magmatic zone. The igneous rocks of Rum comprise early felsic magmas, that are cross-cut by later plutonic ultrabasic to basic Layered Suite (Emeleus, 1997). The felsic magmas are considered to originate from melting of gneissic crust (Troll, Donaldson & Emeleus, 2004) by ascending voluminous basic mantle melts. Such associations of 'early felsic–later mafic' rocks have also been recovered in cores of ocean drilling campaigns at the North Atlantic seaward-dipping wedges, for example, at the Vøring Plateau (Norwegian Sea, Hole 642E, ODP Leg 104: Eldholm, Thiede & Taylor, 1987). In Hole 642E, crustal melts (the 'Lower Series', 133 m drilled, total thickness not known) are covered by a 770 m thick sequence of tholeiitic basalts ('Upper Series'). Rum and the Vøring Plateau, however, represent different zonal and temporal evolutionary stages of formation of Volcanic Rifted Margins, and a comparison of crustal melting in these two locations can contribute to a better understanding of the interactions between ascending mantle melts and crust during continental break-up. Geochemical studies of crustal melts formed during continental break-up have other merits as well. The radiogenic isotopic compositions and trace element patterns of felsic crustal melts and mixtures of basic and felsic magmas are potentially very useful to identify the crustal components involved in melting and mixing, which in turn may provide information on the depth of melting and the make-up of inaccessible crustal layers at the regional or local scale. This paper focuses on a study of the samples from the Isle of Rum. Detailed results of samples from Vøring Plateau, ODP Leg
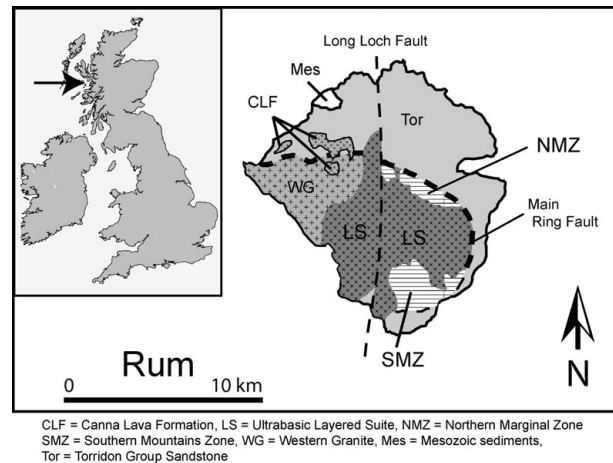
104, Hole 642E are reported elsewhere (Meyer *et al.* 2009).

2. Geological setting and previous work

The varying igneous rock types observed and described from the Isle of Rum have greatly contributed to the development of modern views of the magmatic, as well as the temporal and structural evolution of the British Palaeogene Igneous Province (Bailey, 1945; Emeleus, 1997; Emeleus & Bell, 2005; Troll, Donaldson & Emeleus, 2004; Troll *et al.* 2008). Rum is located on the Hebridean Terrane in NW Scotland (Fig. 2). The igneous centre of Rum was emplaced at around 60.5 Ma (Hamilton *et al.* 1998), most likely in a relatively short period of time (about 500 000 years) (Troll *et al.* 2008). An elliptical ring fault, 12 km across, bounds the igneous centre and marks the remnants of a caldera rim. Major volcanic activity on the Isle of Rum started with the eruption of felsic magmas consisting of extrusive rhyodacitic ignimbrites (about 100 m thick; total eruptive volume estimated at 10 km³: Troll, Emeleus & Donaldson, 2000), and various dacitic to rhyolitic shallow-level intrusions that are all located close to the ring fault. The units of this early felsic phase of activity are cross-cut by basic and ultrabasic layered intrusions (gabbroic and peridotitic rocks) that form the famous Rum ultrabasic Layered Suite (LS), which is effectively a cumulate intrusion (Emeleus, 1997). Small (< 1 m down to 10 cm width) picritic dykes (Upton *et al.* 2002) were intruded at a late stage in the evolution of the Rum basic–ultrabasic complex. Pre-dating both phases is the intrusion of a very coarse gabbro, now preserved as large blocks within some of the early felsic intrusions.

The Palaeogene volcanic and sub-volcanic rocks of Rum intrude an Archaean Lewisian gneiss basement overlain by Proterozoic (Torridon Group) and Mesozoic sediments (Emeleus, 1997). The Archaean Lewisian Gneiss Complex has experienced several

episodes of high-grade metamorphism producing, in this part of Scotland, geochemically distinct lower crustal granulite-facies and upper crustal amphibolite-facies gneisses during its long and often complex geological history (Dickin, 1981; Weaver & Tarney, 1981; Thompson *et al.* 1982; Kinny, Friend & Love, 2005; see Park, Stewart & Wright, 2002, for a full review of the Lewisian). The Lewisian gneiss occurrences on Rum are confined to small outcrops within the Main Ring Fault zone. They are amphibolite-facies gneiss and comprise basic amphibolite gneiss through tonalitic to granodioritic varieties (Emeleus, 1997). Compared to the mainland banded Lewisian gneisses, most of the gneisses on Rum have undergone intense thermal metamorphism as a consequence of the Paleocene magmatism (Tilley, 1944). The overlying Torridon Group and Mesozoic rocks on Rum do not generally show such thermal metamorphism, apart from a few spectacular cases of contact metamorphism close to magmatic plugs and dykes (Holness, 1999; Holness & Isherwood, 2003).

3. Samples and analytical methods

Most of the samples from the Isle of Rum were collected in the Northern Marginal Zone (NMZ), which is a remnant of the rim and infill of a caldera. The Northern Marginal Zone has been studied in depth by Troll, Donaldson & Emeleus (2004). A few samples from the Southern Mountains Zone (SMZ) have been included for comparison. Four samples from 'Unit 9' of the Layered Suite and one sample of a picrite dyke have been analysed to shed light on the relationship between the earliest felsic volcanic products on Rum and the Layered Suite. Three Lewisian gneiss samples from Rum have been selected to serve as analogues for the isotopic and trace element composition of local Lewisian crust.

The sampled igneous rocks include rhyodacites (UDPN; iRDP1; iRDP2; RDP12, Am-iRDP-05), microgranites (LLG; PG3; R-WG-3), dacites (NMZ-AM-7; SMZ-AM-5), basic margins to rhyodacite (SMZ-iRDPBM) and to the dacite (NMZ-AM-Bm). In addition, two pre-Layered Suite basic porphyry dykes (R-FDP-03-M; R-FDP-03-C) from the vicinity of the Layered Suite and two pre-Layered Suite gabbros from within the Am Màm Breccia (R-AMGB-1; R-AMGB-2) were analysed. The reader is referred to Figure 1 of Troll, Donaldson & Emeleus (2004) for detailed information on the local geology and volcanic stratigraphy. Peridotite P-U9, troctolite/allivalite A-U9, and pyroxene–gabbro PxG-UG are samples from Unit 9 of the Layered Suite. Picrite M9 is a sample from a late-stage, thin (10–20 cm wide) olivine–phyric mafic dyke (Upton *et al.* 2002). The gneiss dataset comprises the samples R-GN-1, SR321B and SMZ-AMG-01. The provenance and locality (UK Grid coordinates) of the samples are listed in Table 1. Petrographical descriptions and major-element and mineral compositions of this sample set and similar

rocks from Rum can be found in Emeleus (1997) and Upton *et al.* (2002).

Samples were prepared for chemical analysis at Trinity College, Dublin. Powders were ground in a Tema® tungsten carbide mill, but were unfortunately severely contaminated with W, Co and Ta. Results for these elements are hence not reported in the data table.

Trace elements were determined by a microwave acid digestion procedure and Inductively Coupled Plasma Quadrupole Mass Spectrometry (ICP-MS) at Leuven University (J. Mareels, unpub. Ph.D. thesis, Univ. Leuven, 2004). Sample powder aliquots of 100 mg were dissolved in a mixture of 6 ml 29M HF and 2 ml 14M HNO_3 in high-pressure PTFE vessels in a Milestone Ethos900® microwave digestion system. The vessels were kept at 180 °C for 30 minutes, and at 210 °C for 10 minutes. After addition of 1 ml of In and Re or Tl monitor solutions, the sample solutions were brought to near-dryness to evaporate the largest part of the HF acid and to expel Si as volatile SiF_4. Residues were taken up in 1 ml of 11M $HClO_4$ and 1 ml of a saturated HBO_3 solution in water, and evaporated again. All evaporations were carried out in a Milestone Vacuum Scrubber® unit attached to the microwave digestion system. Finally, the residues were taken up in 10 ml of 14M HNO_3 by heating in closed vessels at 120 °C for 30 minutes. The solutions were quantitatively transferred to a PMP volumetric flask of 250 ml and diluted with ultrapure 18.2 MΩ water. HF and HNO_3 acids were purified by sub-boiling in a PTFE distillation unit. The perchloric acid was commercially available ultrapure acid. Calibration was performed by analysing international reference silicate rocks BCR-2, AGV-1 and BE-N, and by analysing control solutions prepared from commercially available stock solutions. Microgabbro reference rock PM-S was analysed as a control sample. All reference rocks were digested and measured in the same way as rock samples from Rum. The solutions were measured with a HP-4500® ICP-Mass Spectrometer, equipped with a standard Babington nebulizer. Judging from the cross-analysis of the reference rocks, the analysis of rock PM-S, and the duplicate analysis of the picrite sample M9 (Table 2), accuracy is estimated to be better than 10 % relative for most elements. Instrumental precision was variable depending on concentration level.

Isotopic ratios of Sr and Nd were determined at the Scottish Universities Environmental Research Centre (SUERC), East Kilbride, Scotland. Samples were accurately weighed into PFA screw-top beakers (Savillex®) and were dissolved using ultra-pure reagents in a HF–HNO_3–HCl digestion sequence. Sr was separated in 2.5M HCl using Bio-Rad® AG50W X8 200–400 mesh cation exchange resin. A rare-earth-element (REE) concentrate was collected by elution of 3M HNO_3. Nd was separated in a 'cocktail' of acetic acid (CH_3COOH), methanol (CH_3OH) and nitric acid (HNO_3) using Bio-Rad® AG1×8 200–400

Table 1. Results of isotope analysis and trace element analysis of samples from the Isle of Rum

Sample ID	A-U9	P-U9	PxG-U9	M9	R-AMGB-1	R-AMGB-2	R-FDP-03-M	R-FDP-03-C
Rock type	Troctolite	Peridotite	Pyrox-gabbro	Picrite	Gabbro	Gabbro	Basic porphyry	Basic porphyry
Provenance	LS-Unit 9	LS-Unit 9	LS-Unit 9	Post LS-dyke	NMZ-pre-LS	NMZ-pre-LS	NMZ -dyke	NMZ-dyke
UK Grid NM	3924 9728	3923 9728	3922 9728	353 984	38548 98617	38557 98617	38176 9885	38176 9885
$^{87}Sr/^{86}Sr$	0.70372	0.70393	0.70376	0.70281	0.71020	0.70992	0.70670	0.70457
$^{143}Nd/^{144}Nd$	nd	nd	nd	0.51313	0.51210	0.51186	0.51310	0.51305
Sc	4.5	20.7	60.0	18.9	15.3	32	47	37
V	28	56	154	137	189	130	321	259
Cr	2934	4012	2829	3073	13	102	280	134
Ni	338	1999	297	2000	69	36	108	92
Rb	0.39	0.23	0.30	1.32	3.4	3.5	27.9	5.3
Sr	290	55	142	76	347	405	228	245
Y	0.75	1.6	4.5	7.4	3.7	6.8	20.5	18.0
Zr	3.2	3.5	10.4	25.6	9.9	14.0	69.6	68.2
Nb	< 0.3	0.31	0.21	0.62	0.30	0.60	1.21	1.31
Cs	0.007	0.048	0.010	0.024	0.41	0.16	0.98	0.43
Ba	12	2	9	5	60	57	62	13
La	0.52	0.20	< 1.5	1.47	< 0.7	1.79	2.34	2.32
Ce	1.18	0.59	2.23	4.37	2.83	4.37	8.44	7.46
Pr	0.16	0.10	0.39	0.74	0.42	0.65	1.55	1.42
Nd	0.73	0.59	2.29	3.87	1.98	3.36	9.10	8.13
Sm	0.18	0.23	0.75	1.16	0.54	0.99	3.02	2.69
Eu	0.17	0.10	0.30	0.40	0.46	0.61	1.15	0.99
Gd	0.16	0.26	0.87	1.31	0.60	1.16	3.62	3.03
Tb	0.023	0.044	0.16	0.23	0.11	0.23	0.68	0.58
Dy	0.14	0.28	0.94	1.37	0.66	1.25	3.94	3.39
Ho	0.026	0.055	0.18	0.27	0.14	0.26	0.78	0.68
Er	0.071	0.15	0.47	0.76	0.39	0.68	2.13	1.84
Tm	0.010	0.024	0.072	0.11	0.066	0.10	0.33	0.28
Yb	0.064	0.14	0.37	0.65	0.39	0.55	1.81	1.55
Lu	0.010	0.023	0.052	0.10	0.056	0.08	0.26	0.23
Hf	0.095	0.13	0.43	0.80	0.30	0.45	1.98	1.83
Pb	0.31	0.04	0.65	0.48	1.49	< 0.8	2.0	< 0.6
Th	0.03	0.02	0.05	0.06	0.11	0.14	0.11	0.07
U	< 0.01	< 0.01	< 0.01	< 0.01	0.02	(0.01)	0.03	0.02

Sample ID	SMZ-iRDPBM	NMZ-Am-Bm	NMZ-AM-7	SMZ-AM-5	Am-IRDP-05	RDP12	iRDP1	iRDP2
Rock type	Basic margin	Basic margin	Dacite	Dacite	Rhyodacite	Rhyodacite	Rhyodacite	Rhyodacite
Provenance	SMZ rhyodacite	NMZ dacite	NMZ	SMZ	NMZ	NMZ	NMZ	NMZ
UK Grid NM	38455 93551	38811 98560	38739 98598	38217 92353	38220 98449	39659 94028	38407 93736	38285 93437
$^{87}Sr/^{86}Sr$	0.71015	0.71160	0.71405	0.71205	nd	0.71445	0.71366	0.71216
$^{143}Nd/^{144}Nd$	0.51210	0.51207	0.51159	0.51158	nd	0.51128	0.51133	0.51129
Sc	39	37	12.4	15.2	7.4	9.8	11.0	11.6
V	423	370	82	103	11	13	28	22
Cr	36	38	53	42	4	7	35	8
Ni	32	26	32	29	< 4	2	8	4
Rb	17.6	26.5	78	68	94	99	81	70
Sr	269	301	471	467	181	210	239	250
Y	28.2	28.9	18.9	22.8	27.4	32.0	26.3	31.0
Zr	136	127	79	174	237	266	233	272
Nb	8.0	4.0	5.9	8.1	8.3	7.6	9.1	10.8
Cs	0.49	0.37	1.92	1.22	0.92	0.78	0.84	0.76
Ba	238	322	877	1055	1023	920	1052	940
La	14.6	17.6	32.6	35.9	48.8	48.8	44.4	49.2
Ce	33.3	38.1	67.2	69.9	101	95.8	89.4	96.1
Pr	4.6	5.1	8.2	8.8	11.9	12.0	10.7	11.5
Nd	20.7	22.7	31.2	34.7	45.7	44.6	41.0	45.0
Sm	5.1	5.5	5.7	6.3	8.3	8.1	7.4	8.3
Eu	1.60	1.67	1.33	1.62	1.99	1.97	1.82	2.19
Gd	5.2	5.6	4.6	5.3	7.2	7.0	6.1	7.0
Tb	0.93	0.96	0.70	0.83	1.01	1.07	0.94	1.06
Dy	5.4	5.4	3.68	4.4	5.7	5.7	4.9	5.6
Ho	1.09	1.07	0.74	0.87	1.05	1.10	0.95	1.09
Er	2.87	2.97	2.02	2.40	2.98	3.00	2.64	2.96
Tm	0.43	0.44	0.32	0.37	0.41	0.44	0.40	0.46
Yb	2.47	2.56	1.83	2.16	2.65	2.56	2.34	2.60
Lu	0.35	0.38	0.27	0.32	0.40	0.37	0.35	0.39
Hf	3.7	3.5	2.2	4.6	6.9	6.5	5.8	6.8
Pb	2.5	5.2	12.9	8.9	15.4	13.6	8.5	10.3
Th	1.79	2.4	5.5	4.8	7.3	7.1	6.4	6.3
U	0.37	0.58	1.82	1.48	0.97	1.00	1.11	0.87

Table 1. (*Cont.*)

Sample ID	UDPN	LLG	PG3	R-WG-3	R-GN-1	SMZ-AMG-01	SR321B
Rock type	Rock type	Rhyodacite	Microgranite	Microgranite	Microgranite	Gneiss	Gneiss
Provenance	NMZ	NMZ	NMZ	NMZ	Lewisian	Lewisian	Lewisian
UK Grid NM	393 979	36666 99376	37899 92390	346 986	39393 92946	38511 92482	336 004
^{87}Sr/^{86}Sr	0.71352	0.71252	0.71111	0.71426	0.71541	0.71708	0.71856
^{143}Nd/^{144}Nd	0.51126	0.51129	0.51133	0.51177	0.51135	0.51135	0.51135
Sc	10.7	10.5	7.6	7.8	43	11.8	54
V	16	19	70	6	182	86	192
Cr	13	13	13	9	215	68	176
Ni	1	1	4	2	452	53	122
Rb	83	111	54.0	135	32.1	95	18.7
Sr	221	204	502	107	377	298	349
Y	27.7	34.1	16.4	38.0	31.4	16.0	49.7
Zr	234	179	100	175	89	111	37.8
Nb	7.4	9.9	3.5	10.9	5.5	7.3	12.8
Cs	0.76	0.92	0.91	0.89	1.92	2.25	0.15
Ba	995	935	644	951	268	558	217
La	48.5	49.2	28.7	50.1	32.5	29.9	46.1
Ce	91.3	95.3	55.5	105	79.0	60.6	118
Pr	11.8	12.2	6.3	12.1	10.7	7.2	16.7
Nd	45.2	47.2	23.9	47.1	46.0	26.6	71.5
Sm	8.19	8.68	4.27	9.28	9.79	4.63	14.9
Eu	2.17	2.04	1.35	1.64	1.58	1.05	2.64
Gd	6.9	7.6	3.7	8.1	8.17	3.75	12.3
Tb	1.05	1.15	0.57	1.30	1.22	0.57	1.89
Dy	5.6	6.1	3.0	7.3	6.1	2.99	9.6
Ho	1.11	1.19	0.58	1.40	1.10	0.58	1.78
Er	2.97	3.19	1.55	3.86	2.76	1.61	4.8
Tm	0.44	0.47	0.23	0.60	0.41	0.25	0.70
Yb	2.58	2.61	1.32	3.53	2.33	1.45	4.02
Lu	0.38	0.38	0.19	0.49	0.33	0.22	0.57
Hf	6.2	4.5	2.9	5.8	2.5	3.0	1.6
Pb	13.1	11.9	10.9	13.9	12.8	5.9	4.4
Th	5.4	6.6	6.6	9.0	5.7	5.3	2.9
U	0.65	0.76	1.67	1.59	7.8	0.97	0.15

LS – Rum Layered Suite; NMZ – Northern Marginal Zone; SMZ – Southern Mountains Zone
nd – not determined; ( ) – semiquantitative result. Trace element concentrations listed as μg/g (ppm).
Isotopic ratios are age corrected to 60.5 Ma.

mesh anion exchange resin. Total procedure blanks for Sr and Nd were less than 0.5 ng. In preparation for mass spectrometry, Sr samples were loaded onto single Re filaments with phosphoric acid. The Sr samples were analysed on a VG Sector 54–30® multiple collector mass 200 spectrometer. A ^{88}Sr intensity of 1V $(1 \times 10^{-11}$ A) ± 10 % was maintained. The ^{87}Sr/^{86}Sr ratio was corrected for mass fractionation using ^{86}Sr/^{88}Sr = 0.1194 and an exponential law. The mass spectrometer was operated in the peak-jumping mode with data collected as 15 blocks of 10 ratios. NBS987 gave 0.710257 ± 18 (2 SD, n = 14). Nd samples were analysed on a VG Sector 54–30® instrument. ^{143}Nd/^{144}Nd ratios were measured with a ^{144}Nd beam of 1V $(1 \times 10^{-11}$ A). Twelve blocks of 10 ratios were collected in the peak jumping mode and corrected for mass fractionation using an exponential law and ^{146}Nd/^{144}Nd = 0.7219. Repeat analyses of the internal laboratory standard (JM) gave ^{143}Nd/^{144}Nd = 0.511511 ± 9 (2 SD, n = 21). All isotope ratios were age corrected to 60.5 Ma according to the time of igneous eruption and emplacement of the Rum Igneous Centre (Hamilton *et al.* 1998; Troll *et al.* 2008). The isotopic data are listed in Table 1.

4. Geochemistry of the various units

4.a. Sr and Nd isotopic composition

Figure 3 shows the variation of Sr and Nd isotopic compositions in the Rum samples; all isotopic ratios are age corrected to 60.5 Ma. This figure is the framework for the further discussion of the petrogenetic relationships among the samples. The felsic components of the Rum Marginal Zone have high ^{87}Sr/^{86}Sr (0.711–0.715) and low ^{143}Nd/^{144}Nd ratios (0.511–0.513), and all plot close to the composition of Lewisian amphibolite gneisses. The basic margins of the rhyodacites and the pre-Layered Suite gabbros are positioned on an apparent mixing line of rhyodacites and primitive mantle components of the mafic Layered Suite. The basic dykes in the Marginal Zone are enriched in radiogenic Sr (^{87}Sr/^{86}Sr = 0.7046–0.7067) relative to the most primitive LS end-member, but have only marginally lower ^{143}Nd/^{144}Nd ratios. This might point to hydrothermal alteration with Sr-rich and REE-poor fluids.

All the rhyodacites and two out of the three microgranites analysed have a Nd isotopic composition indistinguishable from that of the regional crust and high Sr-isotopic ratios typical of middle crustal material.

Table 2. Trace element analyses of picrite M9 and reference rock PM-S: comparison with literature data

Sample ID Rock type	M9 Picrite			PM-S Microdiorite reference rock	
	Analysis 1	Analysis 2	Upton *et al.* (2002)	This study	Govindaraju (1995)
Sc	20.5	17.4	11.0	29.0	34
V	139	135	121	167	192
Cr	3073	nd	2137	376	314
Ni	1934	2067	1990	109	115
Rb	1.34	1.30	1.90	0.91	1.00
Sr	75.8	75.2	80.0	245	280
Y	7.7	7.1	6.8	10.7	11.0
Zr	22.4	28.8	32.0	29.2	39.0
Nb	0.50	0.73	0.80	1.12	2.6
Cs	0.021	0.027	nd	0.36	0.35
Ba	5.2	5.3	17	148	148
La	1.50	1.43	1.78	2.59	2.80
Ce	4.48	4.25	4.87	6.47	6.80
Pr	0.76	0.73	0.71	1.04	1.08
Nd	3.97	3.76	3.99	5.49	5.50
Sm	1.25	1.08	1.20	1.79	1.75
Eu	0.42	0.37	0.41	1.03	1.07
Gd	1.40	1.22	1.36	2.00	2.00
Tb	0.23	0.23	nd	0.34	0.36
Dy	1.41	1.33	1.32	2.08	2.00
Ho	0.28	0.27	0.25	0.41	0.42
Er	0.78	0.74	0.72	1.14	1.10
Tm	0.11	0.11	nd	0.16	0.17
Yb	0.66	0.64	0.64	0.96	1.00
Lu	0.10	0.10	0.09	0.14	0.15
Hf	0.79	0.81	nd	1.05	1.12
Pb	0.48	nd	0.90	2.13	2.50
Th	0.062	0.051	0.40	0.03	0.05
U	< 0.01	< 0.01	nd	< 0.01	(0.03)

Trace element concentrations listed as μg/g (ppm). nd – not determined; ( ) – semiquantitative result.

Since the REE and Sr budget of the rhyodacites and microgranites is predominantly of crustal origin, it is conceptually straightforward to assume that these rocks were formed by anatexis of crust, as argued by Troll, Donaldson & Emeleus (2004). An interesting aspect of Figure 3 is the position of the rhyodacites on an apparent mixing line between melts derived from Lewisian amphibolite gneiss and melts from Lewisian granulites. If the rhyodacites are such melt mixtures, interpretation schemes for Rum felsic magmas have to be refined to allow for up to 30 % admixture of granulite, a component previously not identified as a crustal contaminant in studies of the Rum ultrabasic Layered Suite (Palacz, 1985; Palacz & Tait, 1985; Tepley & Davidson, 2003). However, such a conclusion might be premature. The data shown in Figure 3 can also be explained without invoking a granulite mixing component, if the Lewisian amphibolite gneiss is not seen as one single composition but as a group of rocks that is heterogeneous with respect to ^{87}Sr/^{86}Sr ratios.

Modelling of crustal contamination of mantle magmas and mixing of crustal melts often relies heavily, if not exclusively, on isotopic correlation diagrams of the ^{87}Sr/^{86}Sr, ^{143}Nd/^{144}Nd and ^{206}Pb/^{204}Pb–^{207}Pb/^{204}Pb–^{208}Pb/^{204}Pb systems. The primary aim of this exercise is the identification of the end-components involved in the mixing process. This is usually reasonably reliable, since the isotopic ratios are not significantly affected by processes such as partial melting and fractional crystallization. However, this strength can also become a shortcoming, because a petrogenetic model cannot be complete without specifying all the processes that determined the range of absolute abundances and variation trends of major and trace elements. To distinguish among the two models outlined in Figure 3, isotope data alone do not suffice. It is necessary to take into account and to model other geochemical properties of the samples, such as the trace element variation trends displayed in Figures 4 to 10.

4.b. The Layered Suite

The samples from the ultrabasic Layered Suite (LS), which have been studied as representative for the mantle component on Rum, are a collection of plutonic rocks and picritic basalts. The Sr and Nd isotopic ratios (Fig. 3) are among the most 'primitive' (or 'least contaminated') values measured in the Rum Layered Suite (Palacz, 1985; Upton *et al.* 2002). The REE pattern of picrite M9 (Fig. 4a) is virtually identical to that reported by Upton *et al.* (2002). This particular picrite dyke is strongly olivine–phyric cumulate rock (∼ 60 % olivine macrocrysts), which is clearly reflected in the high Ni and Cr concentrations and the overall low REE abundances. A much closer candidate for a
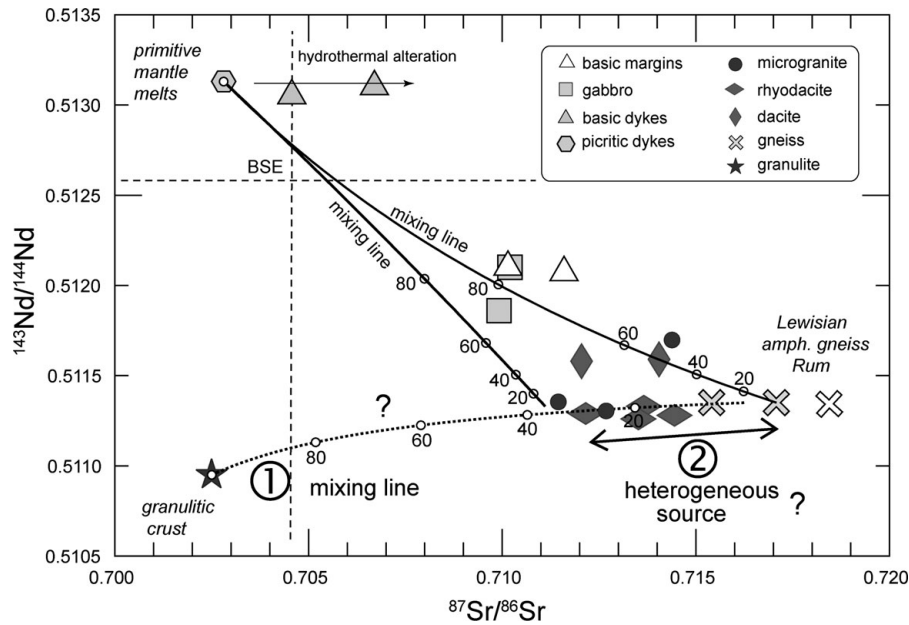
Figure 3. ^{143}Nd/^{144}Nd v. ^{87}Sr/^{86}Sr isotope diagram of Rum igneous rocks and Lewisian crust. The Lewisian granulite crust estimate is from Dickin (1981). Two possible models are outlined. (1) The rhyodacites are binary mixtures between melts derived from Lewisian gneiss and from Lewisian granulite. (2) The rhyodacites are melts from a gneissic crust that is heterogeneous with respect to ^{87}Sr/^{86}Sr. Numbers along mixing lines are mass fractions (in %) of end-members. In both cases, the dacites, pre-Layered Suite gabbros and basic margins of rhyodacites are mixtures between rhyodacitic melts and mafic mantle melts. BSE represents the 'Bulk Standard Earth' estimate. The analytical errors are smaller than the size of the symbols. The data point for the Rum 'primitive mantle melts' is picrite B62/2 of Upton *et al.* (2002). All isotopic data are age corrected to 60.5 Ma.
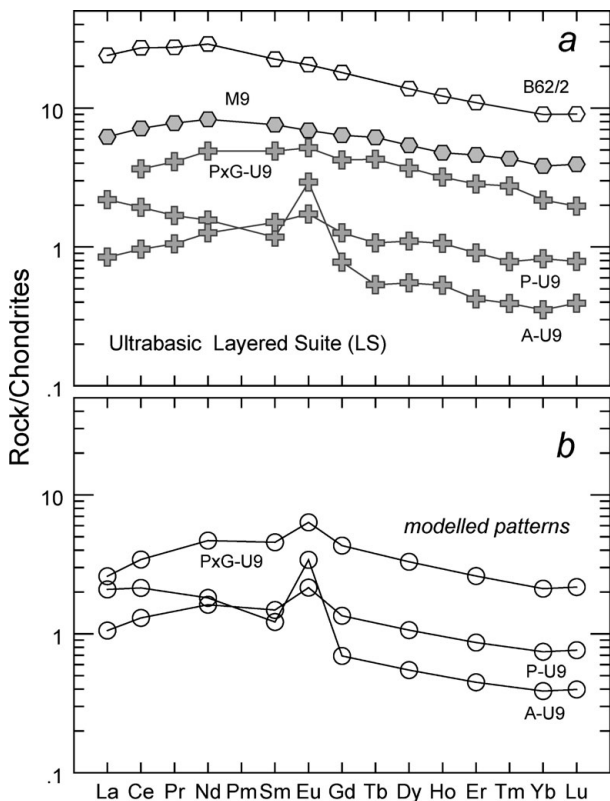
Figure 4. (a) REE patterns of samples from the Rum Layered Suite (LS). Data for picrite dyke B62/2 are from Upton *et al.* (2002). (b) REE patterns of ultramafic rocks modelled as adcumulates after 50 % fractional crystalization of a liquid with REE abundances of picrite B62/2. Parameters of model are listed in Table 3. REE abundances are normalized to C1 chondrite values (Sun & McDonough, 1989).

primitive liquid composition is picrite B62/2 studied by Upton *et al.* (2002), who regarded this sample as representative of a melt composition. Its REE pattern is included in Figure 4a for reference and can be considered as a good approximation ($\pm$ 10 %) of the REE composition of the parental liquid of the Layered Series. The concave-upward REE pattern with a maximum enrichment at Nd, and a slight depletion of La with respect to Ce and Nd, is similar to the primitive 'Transitional-to-Enriched' type tholeiitic basalt that is a common component of the North Atlantic Paleocene Igneous Province.

Although the petrogenesis of the Layered Suite is not the topic of the present paper, a first-order modelling of the cumulate rocks is presented in the next paragraph to show that late-stage basic liquids similar to B62/2 are viable analogues for the melts that formed the Layered Suite and that were the heat engine for crustal melting on Rum.

The very low REE abundances of the troctolite (allivalite) A-U9 and peridotite P-U9 attest to the truly adcumulus nature of the samples and allow for very little trapped intercumulus liquid. REE patterns calculated with a Rayleigh fractionation model of a liquid such as picrite B62/2 are shown in Figure 4b. The cumulus proportions and partition coefficients (calculated from "Geochemical Earth Reference Model – GERM' Database; http://earthref.org) are listed in Table 3. The results shown in Figure 4b are for aggregate cumulate compositions after 50 % crystallization, without any trapped intercumulus liquid. The following equation was used (Neumann, Mead & Vitaliano,

Table 3. Parameters of the fractional crystallization model

	PLAG	CPX	OLIV
Cumulus proportions			
Troctolite LS	0.6	0	0.4
Peridotite LS	0.2	0.1	0.7
PxGabbro LS	0.6	0.4	0
Gabbro NMZ	0.7	0.3	0
Partition coefficients			
La	0.1	0.05	0.01
Ce	0.09	0.1	0.01
Nd	0.07	0.2	0.01
Sm	0.06	0.3	0.01
Eu	0.2	0.3	0.01
Gd	0.04	0.4	0.01
Dy	0.04	0.4	0.013
Er	0.04	0.4	0.015
Yb	0.04	0.4	0.02
Lu	0.04	0.4	0.02

The model applies to the adcumulus rocks from the Layered Suite (Fig. 4) and the pre-LS gabbros (Fig. 6). LS – Rum Ultrabasic Layered Suite; NMZ – Northern Marginal Zone; PLAG – plagioclase; CPX – clinopyroxene; OLIV – olivine. Partition coefficients are a generic set calculated from data in the 'Geochemical Earth Reference Models (GERM) Data Base' (http://earthref.org).

1954):

$$[C_{average\ solid}/C_{initial\ liquid}] = [1/F].[1-(1-F)^D]$$

where C = concentration of trace element i; F = degree of solidification (F = 0.5); $D_i = \Sigma K_{ij} X_j$ = bulk solid/liquid distribution coefficient of trace element i; K_{ij} = solid/liquid partition coefficient of trace element i for mineral j; X_j = crystallization proportion of mineral j (with $\Sigma X_j = 1$). Bytownitic plagioclase dominates the REE patterns in troctolite A-U9 (positive Eu-anomaly; slight enrichment of LREE), while periodotite P-U9 and gabbro PxG-U9 show the imprint of cumulus clinopyroxene (higher HREE and lower LREE). No trapped intercumulus liquid is required to explain the higher REE contents of the pyroxene gabbro.

4.c. The basic members of the Rum Marginal Zones

The two basic porphyry dykes (samples R-FDP-03-M and R-FDP-03-C) from the contact aureole of the Layered Suite in the Northern Marginal Zone have a primitive Nd-isotopic composition (^{143}Nd/^{144}Nd = 0.5131; Fig. 3). The enhanced ^{87}Sr/^{86}Sr ratios (0.7046–0.7067) could be due to hydrothermal activity, as these dykes are heavily altered. However, the prominent La–Ce–Pr–Nd depletion, as compared to picrites B62/2 and M9 (Fig. 5c), is a primary magmatic feature as the REE are immobile during alteration. This is borne out by the smooth and virtually identical patterns of the two analysed samples. The basic dykes most likely represent one member from a range of primitive tholeiitic melts. Similar variations in REE patterns have been observed in successive units of, for example, the Upper Tholeiitic Series drilled during ODP Leg 104 on the Vøring Plateau (Viereck *et al.* 1988, 1989).
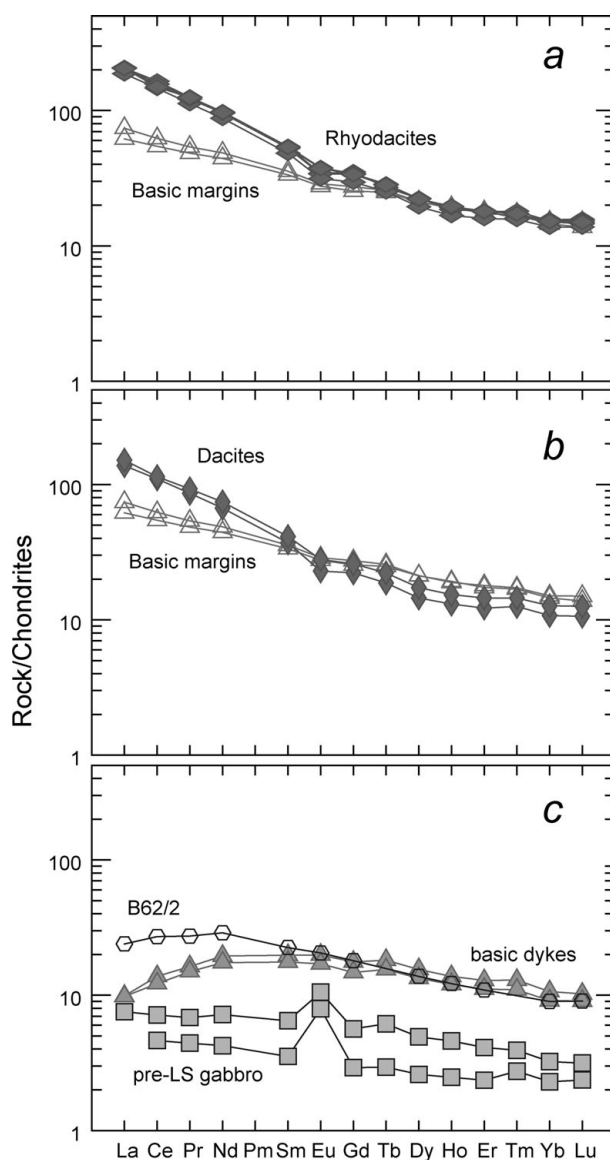

Figure 5. Chondrite normalized REE patterns of (a) rhyodacites, (b) dacites and (c) basic members of the Rum marginal zones. The patterns of the basic margins of the rhyodacite intrusions are included in both (a) and (b) to show the difference between the rhyodacites and dacites. Pattern of picrite B62/2 is repeated in (c) for comparison with patterns of Figure 4. REE abundances are normalized to C1 chondrite values (Sun & McDonough, 1989).

The 'pre-Layered Series' gabbro intrusions (R-AMGB-1 and R-AMGB-2) have REE patterns typical of plagioclase–cumulate plutonic rocks (overall-low REE; positive Eu anomalies; Fig. 5c). These gabbros do not appear to be related to the basic porphyry dykes, because the Sr and Nd isotopic ratios differ greatly (^{87}Sr/^{86}Sr = 0.710; ^{143}Nd/^{144}Nd = 0.512). Moreover, the lack of a depletion of La relative to Nd on chondrite-normalized plots is also an indication that these early gabbros did not crystallize from liquids with a marked La–Ce depletion such as the basic dykes. The similarity of isotopic composition in the gabbros and the basic margins to (rhyo)dacitic intrusions rather suggests that the gabbros crystallized from liquids that were similar
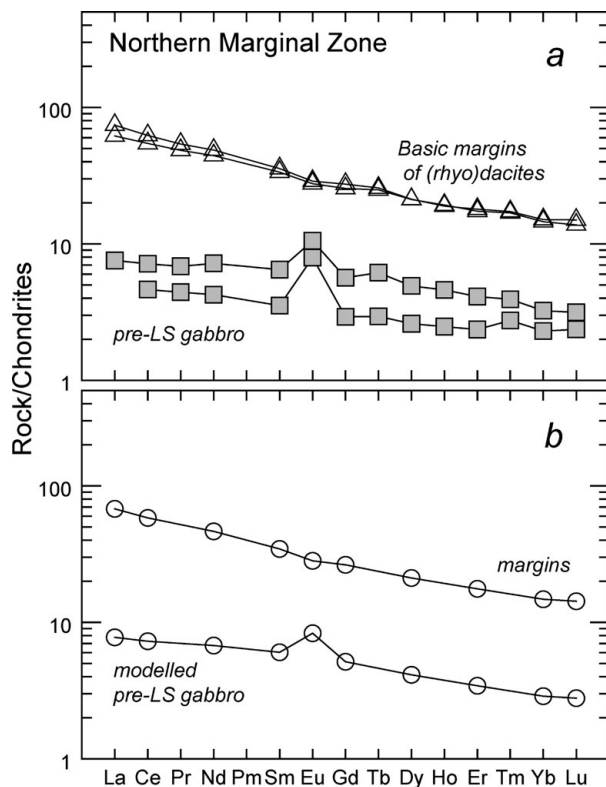
Figure 6. (a) REE patterns of basic margins of (rhyo)dacitic intrusions and the pre-Layered Suite gabbros. (b) REE pattern of pre-Layered Suite gabbro modelled as a 70 % plagioclase–30 % clinopyroxene adcumulate from a liquid similar to that of the basic margins of the rhyodacites. REE abundances are normalized to C1 chondrite values (Sun & McDonough, 1989).

to those that were quenched at the margins. Figure 6b shows that the REE patterns can be modelled quite closely by 50 % crystallization of a 70 % plagioclase–30 % clinopyroxene adcumulate from the margin liquid, using the partition coefficients listed in Table 3, and the fractionation equation listed in Section 4.c.

4.d. The Lewisian amphibolite gneiss samples

Three Lewisian gneiss samples from the Isle of Rum were also analysed. Although the isotopic ratios (Fig. 3) and the shape of the REE patterns (Fig. 7a) are very much alike, there are significant differences in absolute abundances of trace elements, as expected for a petrographically heterogeneous group of rocks. Most Lewisian gneisses cropping out on Rum carry signs of thermal metamorphism (Emeleus, 1997). Fluid loss during reheating could be the main reason for the consistent depletion of the trace elements Rb, Cs, Ba and U in sample SR321B, which was taken from a boulder in the conglomerate that was shed from the dome of the early Rum volcano. In the ensuing discussion, this sample is not considered as representatitve for the composition of the average 'Lewisian gneiss upper crust' beneath Rum. The results of samples R-GN-1 and SMZ-AMG-01 will be used to estimate the range of possible gneiss compositions (indicated by shaded ellipses in Figs 9, 10, 12, 14 and
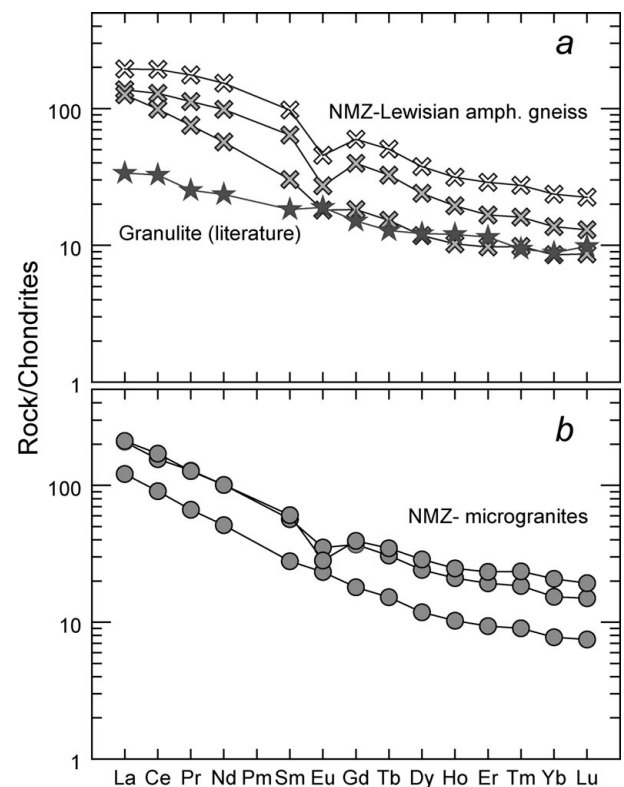
Figure 7. REE patterns of (a) Lewisian amphibolite gneiss and (b) microgranite samples from the Rum Marginal Zone. The granulite pattern is an estimate for an 'average' granulite after Rudnick & Gao (2003). REE abundances are normalized to C1 chondrite values (Sun & McDonough, 1989).
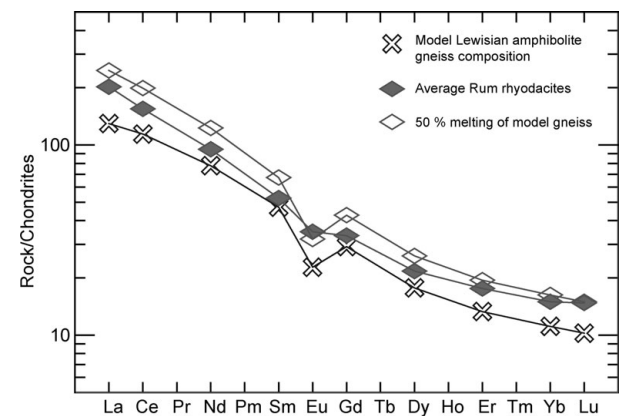

Figure 8. Modelled REE pattern of 50 % partial melts from a model Lewisian amphibolite gneiss (average of samples R-GN-1 and SMZ-AMG-01). A satisfactory match to the rhyodacite patterns can be obtained for degrees of partial melting in excess of 50 %. Parameters of the model are listed in Table 4. REE abundances are normalized to C1 chondrite values (Sun & McDonough, 1989).

15). Figure 7a also displays the REE pattern of an 'average worldwide granulite crust' (Rudnick & Gao, 2003) that has Nd isotopic ratios similar to Lewisian amphibolite gneiss averages. However, the Sr isotopic composition of the granulite is much less radiogenic ($^{87}Sr/^{86}Sr = 0.7025$; Fig. 3) due to evolution in an environment with a low time-integrated Rb/Sr ratio. The average worldwide granulite is generally depleted

Table 4. Parameters of the partial melting modelling of Lewisian amphibolite gneiss (Fig. 8)

	PLAG	KFSP	HBL	QTZ
X_0	0.4	0.2	0.2	0.2
p	0.2	0.4	0.1	0.3
Partition coefficients				
La	0.2	0.1	0.5	0.01
Ce	0.15	0.08	1	0.01
Nd	0.14	0.06	1.5	0.01
Sm	0.12	0.04	2	0.01
Eu	0.4	1	0.5	0.01
Gd	0.08	0.02	2	0.01
Dy	0.08	0.02	2	0.01
Er	0.08	0.02	2	0.01
Yb	0.08	0.02	2	0.01
Lu	0.08	0.02	2	0.01

PLAG – plagioclase; KFSP – alkali-feldspar; HBL – hornblende; QTZ – quartz; X_0– starting modal abundance (mass %) of the minerals; p – fractional contribution of each mineral to the melt.

Partition coefficients are a generic set calculated from data in the 'Geochemical Earth Reference Models (GERM) Data Base' (http://earthref.org).

in LREE and mobile trace elements relative to Lewisian amphibolite gneiss from Rum.

4.e. The dacites, rhyodacites and microgranites

The dacites and rhyodacites have high $^{87}Sr/^{86}Sr$ (0.711–0.715) and low $^{143}Nd/^{144}Nd$ (0.511–0.513) ratios that converge to the values of the Hebridean Lewisian amphibolite gneiss from Rum (Fig. 3). The dacites and rhyodacites have similar REE patterns, but the absolute REE abundances are consistently higher in the rhyodacites than in the dacites (Fig. 5). The rather small variation of abundances indicates that the rhyodacitic and dacitic magmas were homogeneous with respect to REE abundances, in spite of the small though significant variability of Sr isotopic ratios.

The absence of a prominent negative Eu anomaly in a rhyodacite sample led Troll, Donaldson & Emeleus (2004) to conclude that the composition of dacites and rhyodacitic magmas had not been greatly affected by fractional crystallization involving plagioclase. The new analyses show that the absence of a negative Eu anomaly is a persistent feature, and supports their conclusion. The isotopic data and the REE patterns are most readily understood if the dacites and rhyodacites are seen as melts generated by anatexis of crustal material. The most obvious candidate for the parent crustal material similar to the Lewisian amphibolite gneiss was sampled at Rum itself. Figure 8 shows the modelled REE pattern of partial melts of a plagioclase–alkali feldspar–hornblende–quartz gneiss with REE contents of the assumed average Rum amphibolite gneiss (average of samples R-GN-1 and SMZ-AMG-01). The parameters of the non-modal batch melting model (Shaw, 1970) and input data are summarized in Table 4. Although the match between the calculated pattern and the rhyodacite pattern is not perfect, the important point is made that anatexis of gneiss can

produce melts with REE abundances similar to those of rhyodacites, provided that melting proceeded to an extent where little plagioclase or alkali-feldspar was left in the residue, that is, up to at least 50 %. With little constraints on the amounts of water released during melting, it is difficult to decide whether such a high degree of melting is realistic or not. However, one can assume that the temperature of the ascending high-Mg picritic mantle melts that caused crustal anatexis substantially exceeded the solidus temperature of most amphibolite gneiss assemblages. The presence of a negative Eu anomaly in the calculated REE pattern is admittedly a reason for concern about the validity of the model. However, one should take into account that the theoretical equilibrium batch melting equation assumes that part of the Eu^{2+} released in the melt phase by melting of plagioclase + feldspar is repartitioned instantaneously into the residual plagioclase + feldspar fraction. If allowance is made for slow back-diffusion of Eu^{2+} into residual solids, one can expect a smaller negative Eu-anomaly in the partial melts than predicted by the equilibrium model.

The microgranitic intrusions of the Northern Marginal Zone (Fig. 7b) have isotopic ratios and REE patterns that overlap with those of the dacites and rhyodacites. The greater variability of absolute REE abundances is not unexpected for rocks that did not rapidly congeal, but passed through a slower cooling and solidification process. Substantial variation of trace-element concentrations on the hand-specimen or even outcrop scale can result from local fluctuations in ratios of cumulate minerals to interstitial liquid, and from mobility of water-rich residual fluids. In the further discussion it is assumed that these microgranites are plutonic equivalents of the dacites and rhyodacites (Dunham, 1968).

4.f. Ranges of other incompatible trace elements

So far the discussion has focused on the REE elements. Figures 9 and 10 show the ranges and variation trends of other incompatible trace-elements as a function of LREE content, as represented by the Ce data.

The elements Zr, Th, Ba and Rb (Figs 9, 10) follow the general trend of the LREE. Concentrations in the rhyodacites are higher than in the Lewisian gneiss, while dacites have similar or slightly higher contents than the gneiss. The contents of the three microgranites are scattered, but overlap with those of the rhyodacites and dacites. The rhyodacites form a rather homogeneous group, and for most elements the average contents of rhyodacites and dacites are distinctly different. The basic margins to (rhyo)dacites are intermediate between the rhyodacites and the picritic liquids of the Layered Series.

The trace element Cs (Fig. 10) quite unexpectedly shows a different behaviour. In silicate systems this element is present as the Cs^+ species, which is the cation with the largest ionic radius. This element shows
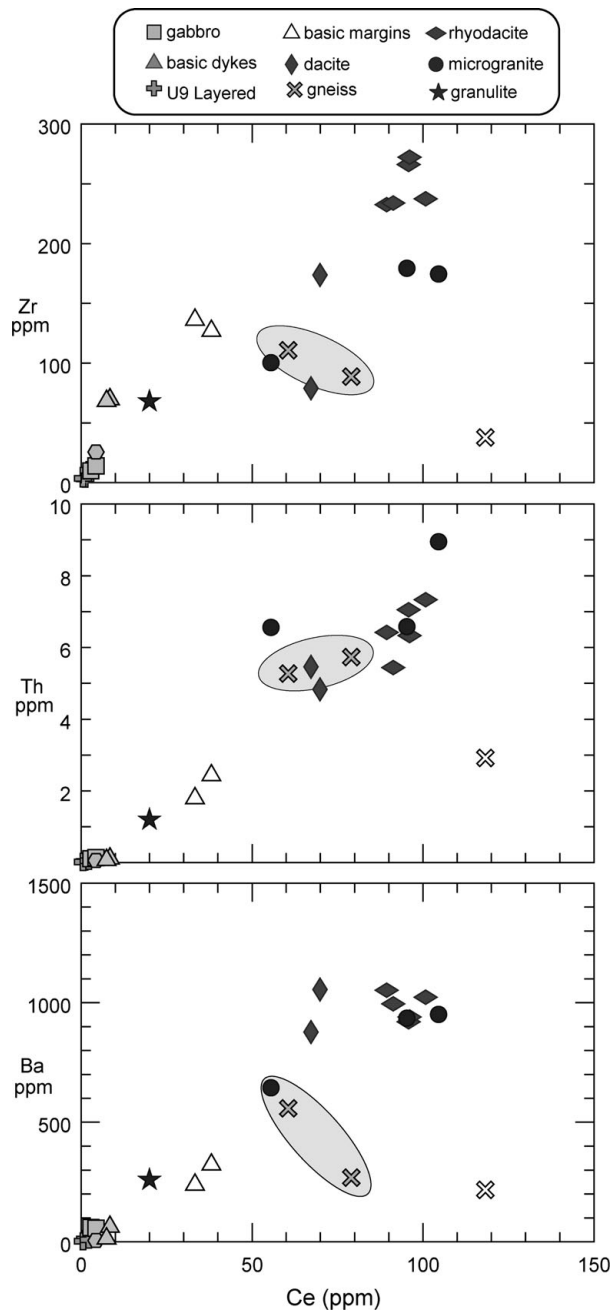
Figure 9. Trace element variation trends of Rum igneous rocks. The shaded ellipse is an estimate of the concentration range of average Lewisian gneiss. Gneiss sample SR321B falls outside this range. Granulite data (star) from Rudnick & Gao (2003).
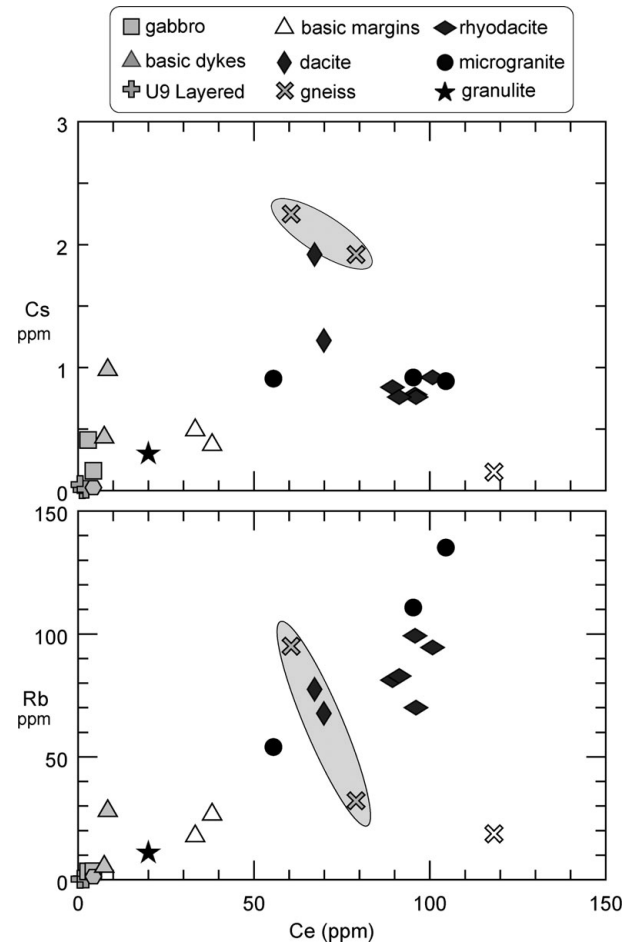

Figure 10. Variation of Cs, Rb and Ce in igneous rocks from Rum. The consistently low Cs contents of the rhyodacites are remarkable.

the greatest contrast in abundance between pristine mantle material, primary mantle melts (< 0.1 ppm), lower crust (0.3 ppm) and especially upper crust (4.9 ppm) (Rudnick & Gao, 2003). The range in concentrations spans 2.5 orders of magnitude. The strong enrichment in the crust, and as a corollary, the strong depletion in depleted mantle, is primarily due to the large size of the Cs^+ ion, which severely limits substitution in most rock-forming minerals, including the common accessories (apatite, zircon, etc.) There is, however, ready substitution for K^+ in micas and, to a lesser extent, in K-feldspar. One would expect

that Cs would be very strongly enriched in the liquid during melting of a gneiss rock, unless micas behaved as refractory residual phases during anatexis. The latter assumption is unlikely to be correct.

It is highly improbable that the low Cs concentrations in the rhyodacites might be due to analytical error. The data for the rhyodacites are very consistent, and have been obtained in two different analytical runs. Furthermore, the duplicate analyses of picrite M9 agreed well, at a concentration level ten times lower than in the rhyodacites. It is equally improbable that Cs was lost from the rhyodacites by hydrothermal alteration. Minor alteration of volcanic glass or K-feldspar would produce secondary phases (sericite, zeolites, etc.) that are as good or even better host phases for Cs^+ as compared to the original magmatic phases. Removal of Cs^+ to the extent observed in the rhyodacites would require extensive alteration in a regime of high water/rock ratios. However, this is ruled out by the petrographical characteristics of rhyodacites, for example, preservation of glass shards and delicate fiamme structures (Troll, Donaldson & Emeleus, 2004).
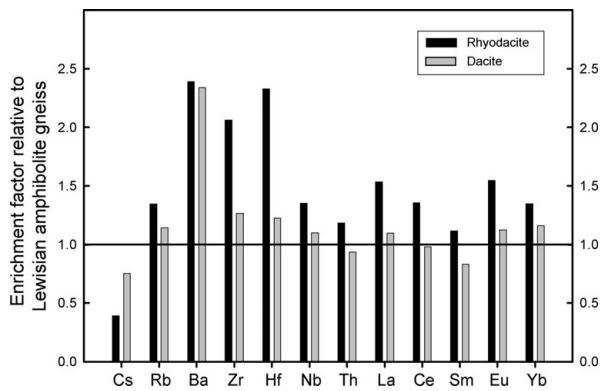
Figure 11. Enrichment or depletion factors of trace elements in rhyodacites and dacites relative to the adopted Lewisian amphibolite gneiss average. Note the lack of a Rb enrichment and in particular the substantial depletion of Cs.

5. Crustal melting and mixing involving Cs–Rb depleted Lewisian amphibolite gneiss

5.a. Indications of Cs–Rb depletion of amphibolite gneiss

Figure 11 shows the enrichment of lithophile trace elements in rhyodacites and dacites with respect to the assumed average Rum Lewisian amphibolite gneiss composition (average of samples R-GN-1 and SMZ-AMG-01). For most of the elements the enrichment factors of the rhyodacites are as expected for substantial crustal anatexis ($\sim$ 30–50 %), taking into account that some lithophile trace elements (e.g. heavy REE) become less incompatible in felsic silicate systems (Mahood & Hildreth, 1983). The high Ba content and lack of a negative Eu anomaly in the rhyodacites indicate that little alkali-feldspar remained in the residual source. The enrichment factors of the dacites are generally smaller than for the rhyodacites. This either points to a higher degree of melting of gneiss, melting of another gneiss component, or mixing with a mafic component (see position of samples in Fig. 3).

On the basis of known geochemical behaviour, one would have expected that the highly incompatible elements Cs and Rb were enriched by at least a factor of 2.5 in the rhyodacites relative to the amphibolite gneiss. This is obviously not the case. Figure 11 further shows that the depletion of Cs in the rhyodacites is not such an aberration after all, because the enrichment factor of Rb is also much smaller than expected for a highly incompatible element. The depletion of Cs lies neatly on a trend formed by the series Ba–Rb–Cs and can therefore be considered as systematic.

Conceptually, there are two ways to explain the low concentrations of the Rb and Cs in the rhyodacites. In a first model, one can view the rhyodacites as mixtures of partial melts of low-Cs Lewisian granulites with partial melts of Lewisian amphibolite gneiss similar to the analysed samples R-GN-1 and SMZ-AMG-01 from Rum. Such a mixing model is outlined in Figure 12b. It demonstrates that no mixture of melts derived from amphibolite gneiss and granulite is
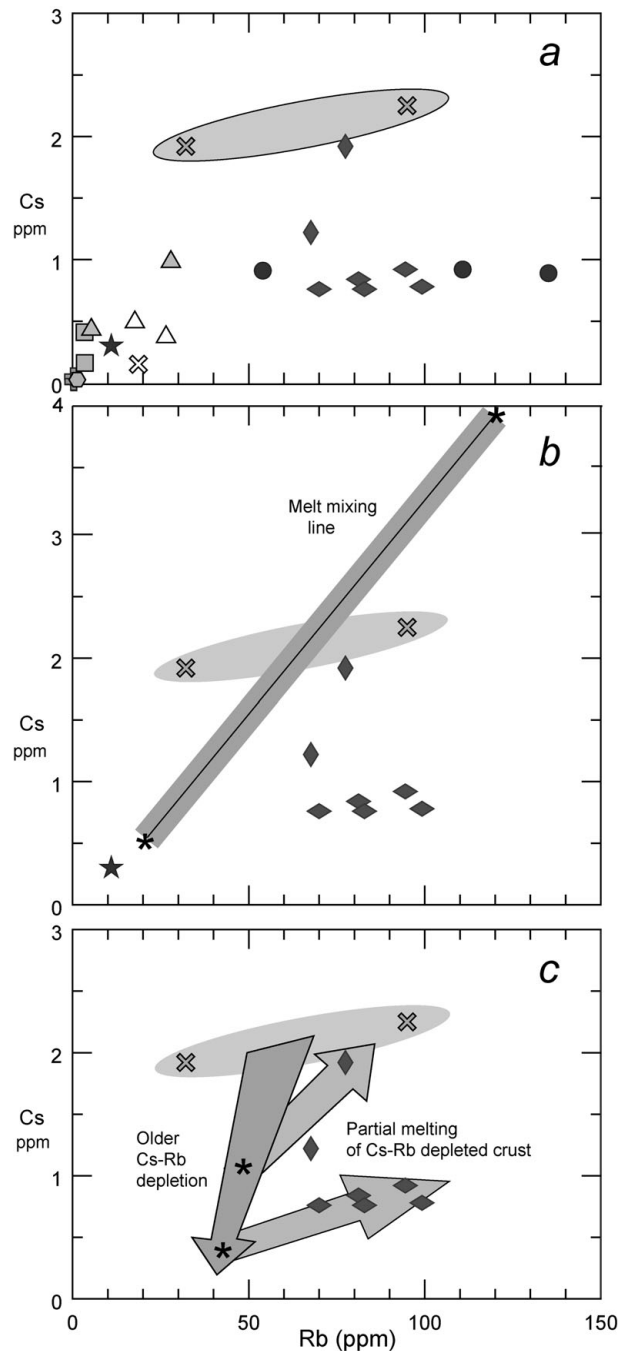

Figure 12. (a) Variation of Cs and Rb in igneous rocks from Rum; sample symbols as in Figures 9 and 10. (b) The mixing line between partial melts of amphibolite gneiss and of granulite does not reproduce the Cs–Rb variation trend of the rhyodacites and dacites. A two-fold enhancement of Cs and Rb in the crustal melts was assumed. (c) Semi-quantitative depletion model of amphibolite gneiss to explain the low Cs and Rb contents of rhyodacites and dacites, which are considered as melts of variably depleted amphibolite crust. If the depletion was an old event, it can account for the variable $^{87}Sr/^{86}Sr$ ratios of the rhyodacites (see Fig. 3).

actually able to reproduce the Cs–Rb variation trend of the rhyodacites and microgranites. A similar conclusion holds with respect to the Cs–Ce variation trend. However, one could argue that the rather flat Cs–Rb trend is brought about by protracted fractional

crystallization of a low-Cs mixed magma that was originally positioned on the mixing line close to the granulite melt end-member. Such an interpretation meets with serious difficulties, because a dominant contribution of melts from granulites to the original melt mixture is not consistent with the position of the rhyodacites close to the amphibolite gneiss end-member in the $^{143}Nd/^{144}Nd$ v. $^{87}Sr/^{86}Sr$ diagram (Fig. 3). Protracted fractional crystallization, with plagioclase and alkali feldspar as the main crystallizing phases, would also generate residual melts with negative Eu-anomalies, which is not the case. Finally, one could altogether question whether straightforward magma mixing is the appropriate mechanism, and argue that the geochemical trends were established by a more complex 'Assimilation Fractional Crystallization' (AFC) process. It is, however, very unlikely that partial melts of lower crustal granulites would have a high enough enthalpy to decompose and assimilate middle-to-upper crustal amphibolite gneiss rock to the extent that the contaminant is dominating the Sr-isotopic composition of the end-product. Here again, the argument about the absence of negative Eu anomalies is pertinent.

A second model to explain the low concentrations of the Rb and Cs in the rhyodacites is based on the assumption that the source of the rhyodacites was similar to the amphibolite gneiss sampled on Rum, except for having been depleted in Rb and Cs prior to the melting event. This model is outlined by the evolution trends shown in Figure 12c. The required depletion for Cs is from ~ 2 ppm to 0.4 ppm. For Rb a smaller depletion from an average value of 60 ppm to 40 ppm is necessary. Partial melting of $\sim 50\%$ would enhance the concentrations to the levels measured in the rhyodacites (~ 0.8 ppm Cs and ~ 80 ppm Rb). Taken at face value, Figure 12 implies that the dacites were formed by melting of lesser Cs and Rb depleted Lewisian gneiss sources. This second model has the advantage of conceptual simplicity, and it readily accounts for the absence of negative Eu anomalies and for the convergence of isotopic composition rhyodacites to the amphibolite gneiss ratios. The model will be examined further in the following Sections.

5.b. Timing and causes of the Cs–Rb depletion

An important aspect of the model is the timing of the assumed depletion process. If it took place concurrently with or within a few millions of years prior to the crustal melting that gave rise to the rhyodacites, the depletion event would have had no consequences for the isotopic composition of the rhyodacites. In order to explain the spread of the $^{87}Sr/^{86}Sr$ ratios and the generally lower ratios of the rhyodacites relative to the amphibolite gneiss, one has to consider two different explanations. (1) The Cs–Rb depleted source regions of the rhyodacite melts were already heterogeneous with respect to $^{87}Sr/^{86}Sr$, and had evolved in an environment with a lower time-integrated Rb/Sr ratio than did the
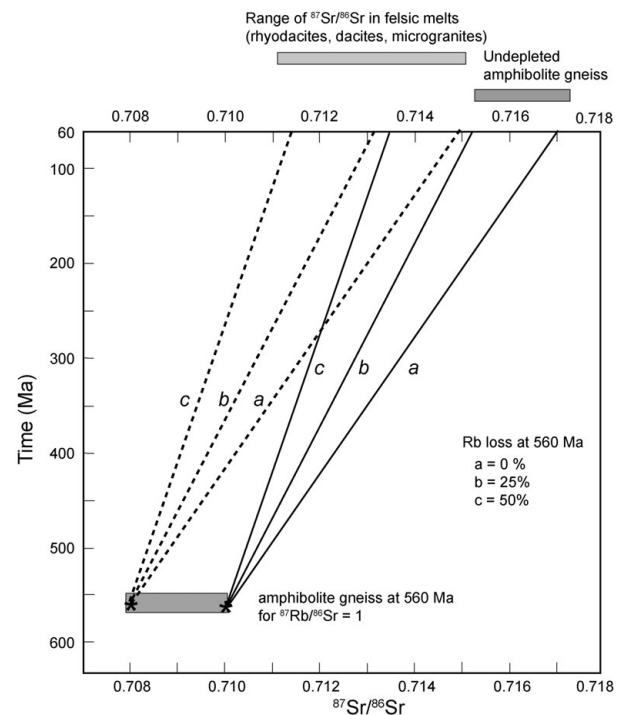

Figure 13. Conceptual model of Sr-isotopic evolution of amphibolite gneiss that underwent variable degree of Rb (and Cs) depletion in the past. Two cases are presented. In the first, the undepleted amphibolite gneiss attains a $^{87}Sr/^{86}Sr$ ratio of 0.717 at 60 Ma, comparable to the high range of amphibolite gneiss sampled at Rum. If such a sample underwent 25 % Rb loss $c.$ 560 Ma ago, it would attain a value $^{87}Sr/^{86}Sr$ ratio of 0.7152 at 60 Ma; with 50 % Rb loss, the ratio would grow to 0.7135. In the second case, the undepleted amphibolite gneiss has a $^{87}Sr/^{86}Sr$ ratio of 0.715 at 60 Ma (low range of amphibolite gneiss on Rum). The depleted samples would cover a $^{87}Sr/^{86}Sr$ range of 0.7113 to 0.7132. The $^{87}Sr/^{86}Sr$ values of depleted samples at 60 Ma corresponds to the observed range in felsic melts from Rum.

analysed amphibolite gneiss sampled from Rum. (2) The rhyodacites are mixtures of melts derived from Lewisian granulites and from Cs–Rb depleted Lewisian amphibolite gneiss having $^{87}Sr/^{86}Sr$ ratios within the same range as the analysed amphibolite gneiss from Rum; the amphibolite gneiss source contributes more than $\sim 70\%$ by mass to the melt mixtures (see Fig. 3).

The situation is different when one assumes that the Cs–Rb depletion took place many tens or even hundreds of millions of years before Paleocene times. Figure 13 shows the effect of an ancient Cs–Rb depletion event on the Sr-isotopic evolution of the potential amphibolite gneiss source regions of the rhyodacites. The graph shows the change back in time of the $^{87}Sr/^{86}Sr$ ratio of two amphibolite gneiss formations, having $^{87}Rb/^{86}Sr = 1$ (a common value for Hebridean amphibolites) and $^{87}Sr/^{86}Sr$ ratios of 0.717 and 0.715 at 60 Ma ago (as for the analysed samples from Rum; Fig. 3). In a second step, one can readily calculate the expected $^{87}Sr/^{86}Sr$ ratios of those two gneiss formations at 60 Ma ago, assuming they had lost between 25 % and 50 % of the Rb at a given moment in the past. The range

of estimated percentage loss of Rb is based on the observed (~ 1.4) and expected (~ 2.3) enrichment of Rb in rhyodacites relative to average amphibolite gneiss (see Fig. 11). Figure 13 indicates that the depleted gneiss formations had at 60 Ma similar ^{87}Sr/^{86}Sr ratios to the rhyodacites, if the depletion event took place somewhere between 400 Ma and 600 Ma before the Paleocene. This time frame obviously makes sense, because it links the inferred Cs–Rb depletion event to Caledonian metamorphism. While Figure 13 is no proof of a Caledonian age of the depletion event, it none the less shows that this time frame and sequence of events is consistent with Sr-isotopic evolution and Cs–Rb data. Admittedly, this time frame is not readily reconciled with the evidence that rocks cropping out in the Hebridean Terrane have not been affected by Caledonian regional metamorphism at *c.* 450 Ma. However, Rum is situated at a distance of only 15 km to the west of the Moine Thrust Belt, the assumed western limit of Caledonian regional metamorphism. In the light of evidence (Kelley, Reddy & Maddock, 1994) for major movements at *c.* 430 Ma even in the Outer Isles Thrust zone about 100 km to the west of the Moine thrust, it is not inconceivable that the Caledonian Moine overthrusting initiated faulting and high-temperature fluid flow (Kerrich, La Tour & Willmore, 1984) in deeper crustal zones at the eastern edge of the Hebridean Terrane.

The other Palaeozoic magmatic episode that affected the Western Scottish Highlands area is the intrusion of Carboniferous–Permian dyke swarms of tholeiitic to alkaline composition (Baxter, 1987), but it is improbable that this event caused regional thermal metamorphism at mid-crustal depths. Although it is commonly assumed that Rb (and by inference Cs) is mobilized by medium- to high-grade regional metamorphism in a suprasubduction environment, the evidence for it is largely indirect and based on such information as resetting of Rb/Sr clocks and the generally low Rb content of granulite facies rocks. However, there is a substantial amount of data from experimental studies of the element mobility from subducted sediments and oceanic crust (e.g. Manning, 2004; Zack & John, 2007; Spandler, Mavrogenes & Hermann, 2007). These experiments demonstrate that Cs and Rb are readily mobilized by water-rich fluids at subsolidus conditions. For completeness, it can be noted that a metamorphic event even at 400–600 Ma ago will not affect the ^{143}Nd/^{144}Nd system, because Nd and Sm contents are not noticeably changed by metamorphism and the time interval is too short compared to the 106 Ga half-life of ^{147}Sm.

5.c. Modelling of the trace element and isotope variation trends

A model for the melting and mixing processes on Rum that takes account ancient Cs–Rb depletion of amphibolite gneiss has one important advantage over other models mentioned above, namely, it accounts
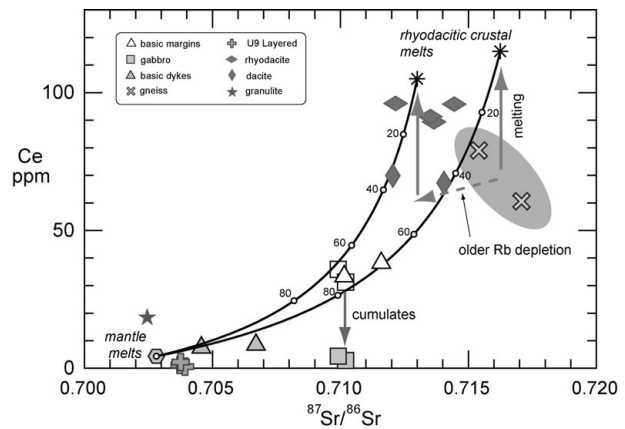

Figure 14. Modelled Ce v. ^{87}Sr/^{86}Sr evolution trend based on the 'older Cs–Rb depletion' model shown in Figure 12c. The granulite component is based on data of Dickin (1981) and Rudnick & Gao (2003). All isotopic data are age-corrected to 60.5 Ma. The rhyodacites are modelled as 50 % melts from a partially Rb depleted Lewisian source; the data allow up to 10 % mixing with mafic mantle melts. The dacites, basic margins and the parent magma of the pre-Layered Suite gabbros are mixtures between mantle melts and Lewisian gneiss melts; see Figure 6 for the modelling of gabbro adcumulates. The numbers along the mixing lines are the mass fraction (in %) of the mafic melt in the hybrid rocks.

for the range ^{87}Sr/^{86}Sr ratios of rhyodacites without invoking a contribution of melts from Lewisian granulites. It would indeed be somewhat unsatisfactory to invoke a substantial mixing component that apparently left no trace as a contaminant of samples from the Rum ultrabasic Layered Suite (Palacz, 1985; Palacz & Tait, 1985; Tepley & Davidson, 2003). In addition, an ancient Cs–Rb depletion provides a causal link between the lower Cs concentrations and the lower ^{87}Sr/^{86}Sr ratios of rhyodacites as compared to the amphibolite gneiss samples. The model is further evaluated in Figures 14 and 15 for its success in consistently reproducing isotopic ratios of Sr and Nd, as well as the absolute concentrations of a typical incompatible lithophile trace element such as Ce. In both figures the enrichment factor of Rb and Ce during crustal melting is set equal to 2, that is, for approximately 50 % partial melting (see Fig. 8). The model explores melt mixing processes only. Arguments against the feasibility of an 'Assimilation Fractional Crystallization' (AFC) model for the the origin of rhyodacites and dacites were given in Section 5.a. Admittedly, AFC could be an acceptable process to model geochemical variations in the basic dykes and early pre-Layered Suite gabbros. However, in view of the petrographical evidence for co-mingling of mafic and felsic magmas in Rum (Troll, Donaldson & Emeleus, 2004), melt mixing was assumed to be the dominant process for all samples.

The position of the rhyodacites and dacites in the Ce v. ^{87}Sr/^{86}Sr diagram (Fig. 14) can be explained by melting of a gneiss that underwent variable Rb depletion. The rhyodacites might be mixed with ~ 10 % basic mantle melts, the dacites with 30 to 45 %. The
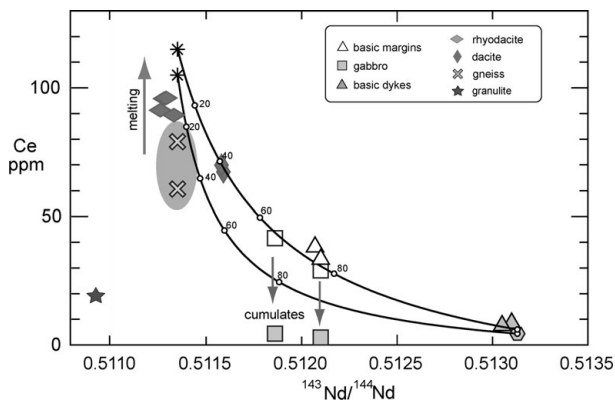
Figure 15. Modelled Ce v. ^{143}Nd/^{144}Nd evolution trend of the of Rum igneous rocks. This diagram does not depend on the gneiss depletion model. The granulite component is based on data of Dickin (1981) and Rudnick & Gao (2003). Two mixing lines between crustal melts from amphibolite gneiss and mafic mantle melts are plotted to show the effect of a range of Ce contents of the gneiss crust and the mantle melts. The mixing estimates are consistent with the values derived in Figure 14. Note that mixing with a melt from a granulite source is not required to explain the position of the dacitic melts in this diagram.

basic margins of the (rhyo)dacites and the pre-Layered Suite gabbro, after correction for cumulate processes (Fig. 6), also plot on the theoretical mixing curves. They can be modelled as mixtures of ∼ 70 % basic mantle melts and ∼ 30 % (rhyo)dacitic melts.

The Ce v. ^{143}Nd/^{144}Nd diagram (Fig. 15) is actually not affected by the Cs–Rb depletion event(s) discussed above. The estimates of crustal or mantle melt contribution to the rhyodacites, dacites, pre-Layered Suite gabbros and basic margins are consistent with the estimates deduced from the Ce–^{87}Sr/^{86}Sr diagam (Fig. 14). Figure 15 clearly shows the differences between the rhyodacites and dacites. The dacites seem to be derived from a less Rb–Cs depleted crustal host rock (Fig. 12) and contain a greater contribution of basic melts. The latter model also offers an explanation for the lower overall REE abundances in the dacites (Fig. 5).

6. Comparison of Rum with other units of the North Atlantic Volcanic Rifted Margins system

Crustal anatexis and the formation of mixtures between mantle and crust melts, either by magma mixing or advanced 'Assimilation Fractional Crystallization' (AFC), appear to be an integral part of igneous processes accompanying the development of Volcanic Rifted Margins. Figure 16 summarizes the ^{87}Sr/^{86}Sr–^{143}Nd/^{144}Nd data for three cases of the North Atlantic Volcanic Rifted Margins: Rum (this work), Vøring Plateau (Viereck et al. 1988; Meyer et al. 2009) and SE Greenland (Fitton et al. 2000). Available data for Skye define a trend that largely coincides with the field of the SE Greenland Lower Series (Carter et al. 1978; Dickin, 1981; Thirlwall & Jones, 1983) and Middle Series (Gibson, 1991). Lewisian average granulite gneiss is
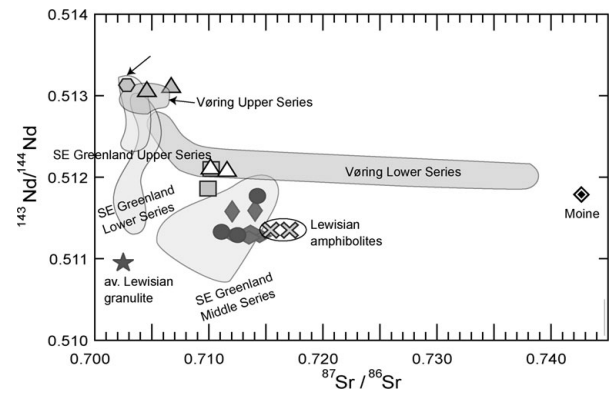

Figure 16. Comparison of the Rum Nd and Sr isotope ratios with available data from North Atlantic Volcanic Rifted Margin units from ODP Leg 152, SE Greenland margin, and from ODP Leg 104, Vøring Plateau, Norwegian Sea. See text for data sources. Symbols of Rum samples are as in Figure 15.

from Dickin (1981). The composition of the 'Moine' meta-psammite is an average of data from Geldmacher et al. (1998); it is included as representative for the isotopic composition of medium-grade metamorphic upper continental crust material.

The isotopic characteristics and major-element chemistry of the Rum rhyodacites and the peraluminous rhyodacites from the Vøring Plateau are an indication that these rocks are essentially melts from crustal material, with perhaps a minor (< 15 %) admixed component of mantle melts. Intermediate rocks (dacites, andesites, gabbros, etc.) represent variable mixtures of crust and mantle derived materials. Only a small fraction of the most mafic picrites, basalts and gabbros represent genuine mantle melts that largely escaped contamination with crustal material.

Rum, Vøring Plateau and SE Greenland represent different spatial/temporal formation stages of the North Atlantic Volcanic Rifted Margin system, and show a remarkably diverse record of mantle–crust interaction processes. The geochemistry of the igneous products is an important source of information on the nature, composition and approximate depth where the main interaction between ascending mantle melts and crust took place. In the case of SE Greenland, crustal anatexis and/or magma mixing of the Lower and Middle Series material most likely proceeded at different depths (granulitic, gneissic). Felsic melts on Rum were largely formed by anatexis of Lewisian amphibolite gneisses, though the inferred Cs–Rb depletion discussed above points to melting of gneisses that were affected by a higher grade of metamorphism than most outcropping gneisses. The indication that on nearby Skye, granulites (Carter et al. 1978; Thirlwall & Jones, 1983) and Lewisian gneisses (Gibson, 1991) have been involved is a reminder that local structure of the crust exerts a substantial control on mantle/crust interaction. Presumably, tectonic and structural factors had a great impact on the nature of mantle/crust interaction on the Vøring Plateau. The seaward-dipping wedges were emplaced on the edge of a thinned and stretched
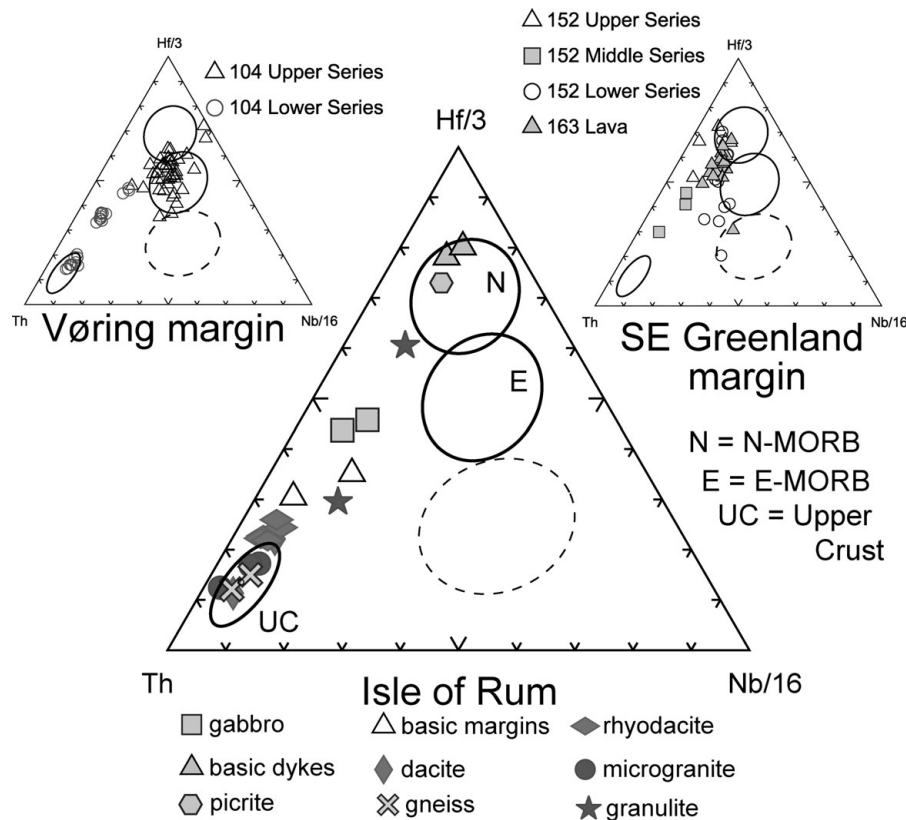
Figure 17. Th–Hf/3–Nb/16 diagram for the representative Rum samples and available data from the seaward-dipping reflector sequences of SE Greenland (Fitton *et al.* 2000) and the mid-Norwegian Vøring margin (Meyer *et al.* 2009). Included in the Rum plot are the average granulite compositions (star symbol) proposed by Wood (1980) and Rudnick & Gao (2003). Felsic rocks from Rum and the Vøring margin extend into the Th-apex, which represents the Upper Crustal end-member. This is not the case for the SE Greenland margin samples. Fields for N-MORB and E-MORB are indicated; the dashed ellipse encloses the field of oceanic island basalts and continental alkaline and tholeiitic basic rocks (Wood, 1980).

extended zone of the continental crust. Therefore, it may be in line with expectations that the crustal component involved in melting at the Vøring Plateau was akin to the psammitic/pelitic Moine schists that represent higher crustal levels in the North Atlantic realm.

The distinct geochemical trends seen in isotopic compositions are also observed for incompatible trace elements. A good illustration is the variation patterns displayed in the Th–Hf/3–Nb/16 ternary diagram (Fig. 17), which is a geochemical analogue of the Th–Hf/3–Ta diagram previously used by Thompson *et al.* (1986) to establish the nature and extent of crustal contamination. Indeed, the Th-apex is the locus of low-to-medium-grade metamorphic crustal rocks, which in a continental break-up environment can either serve as the parent material in crustal anatexis or the contaminant in assimilation–fractional crystallization. The samples from Rum and the Vøring Plateau form an array that starts at the Th-depleted corner with mantle melts and ends at the Th-rich corner with crustal melts. The variation within the SE Greenland series is more complex, but there is an indication that the crustal component involved was a granulite or gneiss that had lost some Th (together with Rb and Cs) during high-grade metamorphism.

Figures 15 and 16 are interesting for other reasons as well. The most primitive and uncontaminated basaltic mantle components from the North Atlantic Volcanic Rifted Margins system have quite homogeneous $^{87}Sr/^{86}Sr$–$^{143}Nd/^{144}Nd$ isotopic compositions, and are in this respect close to the composition of typical North Atlantic MORB. This similarity is underscored by the Th–Hf/3–Nb/16 diagrams. The parent mantle melts in the three cases all plot in the field of primitive N-MORB with some spillover into the E-MORB field, particularly for the Vøring Plateau Upper Series basalts. There is not much of a close affinity with 'within plate' continental basalts.

7. Conclusions

$^{87}Sr/^{86}Sr$ and $^{43}Nd/^{144}Nd$ isotopic compositions together with trace element data reinforce the conclusion of Troll, Donaldson & Emeleus (2004) that the early rhyodacitic volcanic rocks on the Isle of Rum are largely a product of crustal anatexis by ascending mantle melts. Mixing between rhyodacite magma and mafic mantle magmas gave rise to a series of variously mixed dacites, basic dyke margins and gabbros. The parent material of the rhyodacitic melts are Lewisian amphibolitic gneisses. However, the geochemistry of

the strongly incompatible and mobile trace elements Cs and Rb indicates that the amphibolite gneiss parent material had experienced partial loss of Cs and Rb prior to the melting event at *c.* 60.5 Ma ago. The timing of the depletion cannot be determined exactly, but a Caledonian (*c.* 450–550 Ma) age for the Rb depletion can account for the heterogeneity of $^{87}Sr/^{86}Sr$ ratios of the rhyodacites and their lower ratios as compared to amphibolite gneiss sampled at Rum. There is no compelling need to invoke an additional lower-crustal granulitic component to account for the isotopic and trace element variations.

The late-stage picritic melts on Rum are close analogues for the mantle melts that caused crustal anatexis and were the parent melts of the Rum Layered Suite. These mantle melts have close affinities to slightly-depleted to slightly-enriched North Atlantic MORB.

Crustal anatexis is a common process in the rift-to-drift evolution during continental break-up and the formation of Volcanic Rifted Margins systems. Similar associations of 'early felsic–later mafic' volcanic rocks have been recovered from the now-drowned seaward-dipping wedges on the shelf of SE Greenland and on the Vøring Plateau (Norwegian Sea). The felsic–mafic rock associations of the Isle of Rum are an excellent onshore analogue to help to understand the igneous construction of Volcanic Rifted Margins systems. The igneous rocks from Rum, SE Greenland and the Vøring Plateau show geochemical differences that result from differences in the regional crustal composition and the depth at which crustal anatexis took place, but reflect a mafic MORB-type magma end-member that is remarkably similar in all three cases.

References

BAILEY, E. B. 1945. Tertiary igneous tectonics of Rhum, Inner Hebrides. *Quarterly Journal of the Geological Society of London* **100**, 165–91.

BAXTER, A. N. 1987. Petrochemistry of late Palaezoic alkali lamprophyre dykes from N Scotland. *Transactions of the Royal Society Edinburgh: Earth Sciences* **77**, 267–77.

CARTER, S. R., EVENSEN, N. M., HAMILTON, P. J. & O'NIONS, R. K. 1978. Neodymium and strontium isotopic evidence for crustal contamination of continental volcanics. *Science* **202**, 743–7.

COFFIN, M. F. & ELDHOLM, O. 2005. Large igneous provinces. In *Encyclopedia of Geology* (eds R. C. Selley, R. Cocks & I. R. Plimer), pp. 315–23. Oxford: Elsevier.

DICKIN, A. P. 1981. Isotope geochemistry of Tertiary igneous rocks from the Isle of Skye, NW Scotland. *Journal of Petrology* **22**, 155–89.

DUNHAM, A. C. 1968. The felsites, granophyre, explosion breccias and tuffisites of the north-eastern margin of the Tertiary igneous complex of Rhum Inverness-shire. *Journal of the Geological Society, London* **123**, 327–52.

ELDHOLM, O., GLADCZENKO, T. P., SKOGSEID, J. & PLANKE, S. 2000. Atlantic volcanic margins: a comparative study. In *Dynamics of the Norwegian Margin* (ed. A. Nøttvedt), pp. 411–28. Geological Society of London, Special Publication no. 167.

ELDHOLM, O., THIEDE, J. & TAYLOR, E. 1987. *Proceedings of the Ocean Drilling Program, Initial Reports, vol. 104*. College Station, TX (Ocean Drilling Program).

EMELEUS, C. H. 1997. *Geology of Rum and the adjacent islands.* Memoir of the British Geological Survey, Scotland (Sheet 60).

EMELEUS, C. H. & BELL, B. R. 2005. *British Regional Geology: the Palaeogene volcanic districts of Scotland (4th edition)*. Nottingham: British Geological Survey.

FITTON, J. G., LARSEN, L. M., SAUNDERS, A. D., HARDARSON, B. S. & KEMPTON, P. D. 2000. Palaeogene continental to oceanic magmatism on the SE Greenland continental margin at 63°N: a review of the results of Ocean Drilling Program Legs 152 and 163. *Journal of Petrology* **41**, 951–66.

GELDMACHER, J., HAASE, K. M., DEVEY, C. W. & GARBE-SCHÖNBERG, C. D. 1998. The petrogenesis of Tertiary cone-sheeets in Ardnamurchan NW Scotland: petrological and geochemical contraints on crustal contamination and partial melting. *Contributions to Mineralogy and Petrology* **131**, 196–209.

GIBSON, S. A. 1991. The geochemistry of the Trotternish sills, Isle of Skye: crustal contamination in the British Tertiary Volcanic Province. *Journal of the Geological Society, London* **147**, 1071–81.

GOVINDARAJU, K. 1995. 1995 working values with confidence limits for twenty-six CRPG, ANRT and IWG-GIT geostandards. *Geostandards Newsletter (Special Issue July 1995)* **19**, 1–32.

HAMILTON, M. A., PEARSON, D. G., THOMPSON, R. N., KELLEY, S. P. & EMELEUS, C. H. 1998. Rapid eruption of Skye lavas inferred from precise U–Pb and Ar–Ar dating of the Rum and Cuillin plutonic complexes. *Nature* **394**, 260–3.

HOLNESS, M. B. 1999. Contact metamorphism and anatexis of Torridonian arkose by minor intrusions of the Rum Igneous Complex, Inner Hebrides, Scotland. *Geological Magazine* **136**, 527–42.

HOLNESS, M. B. & ISHERWOOD, C. E. 2003. The aureole of the Rum Tertiary Igneous Complex, Scotland. *Journal of the Geological Society, London* **160** 15–27.

KELLEY, S. P., REDDY, S. M. & MADDOCK, R. 1994. Laser-probe $^{40}Ar/^{39}Ar$ investigation of a pseudotachylyte and its host rock from the Outer Isles thrust, Scotland. *Geology* **22**, 443–6.

KERRICH, R., LA TOUR, T. E. & WILLMORE, L. 1984. Fluid participation in deep fault zones: evidence from geological, geochemical, and $^{18}O/^{16}O$ relations. *Journal of Geophysical Research* **89**, 4331–43.

KINNY, P. D., FRIEND, C. R. L. & LOVE, G. J. 2005. Proposal for a terrane-based nomenclature for the Lewisian Gneiss Complex of NW Scotland. *Journal of the Geological Society, London* **162**, 175–86.

MAHOOD, G. & HILDRETH, W. 1983. Large partition coefficients for trace elements in high-silica rhyolites. *Geochimica et Cosmochimica Acta* **47**, 11–30.

MANNING, C. E. 2004. The chemistry of subduction-zone fluids. *Earth and Planetary Science Letters* **74**, 1–16.

MENZIES, M. A., KLEMPERER, S., EBINGER, C. & BAKER, J. 2002. Characteristics of volcanic rifted margins. In *Volcanic Rifted Margins* (eds M. A. Menzies, S. Klemperer, C. Ebinger & J. Baker), pp. 1–14. Geological Society of America, Special Paper no. 362.

MEYER, R., HERTOGEN, J., PEDERSEN, R.-B., VIERECK-GÖTTE, L. & ABRATIS, M. 2009. Interaction of mantle derived melts with crust during the emplacement of the Vøring Plateau, N.E. Atlantic. *Marine Geology*, in press.

MEYER, R., VAN WIJK, J. & GERNIGON, L. 2007. The North Atlantic Igneous Province: A review of models for its formation. In *Plates, Plumes, and Planetary Processes* (eds G. R. Foulger & D. M. Jurdy), pp. 525–52. Geological Society of America, Special Paper no. 430.

NEUMANN, H., MEAD, J. & VITALIANO, C. J. 1954. Trace element variation during fractional crystallization as calculated from the distribution law. *Geochimica et Cosmochimica Acta* **6**, 90–9.

PALACZ, Z. A. 1985. Sr–Nd–Pb isotopic evidence for crustal contamination in the Rhum intrusion. *Earth and Planetary Science Letters* **74**(1), 35–44.

PALACZ, Z. A. & TAIT, S. R. 1985. Isotopes and geochemical investigation of unit 10 from the Eastern Layered Series of the Rhum Intrusion, Northwest Scotland. *Geological Magazine* **122**, 485–90.

PARK, R. G., STEWART, A. D. & WRIGHT, D. T. 2002. The Hebridean Terrane. In *The Geology of Scotland* (ed. N. W. Trewin), pp. 45–80. London: Geological Society.

RUDNICK, R. L. & GAO, S. 2003. The Composition of the Continental Crust. In *The Crust* (ed. R. L. Rudnick), pp. 1–64. Oxford: Elsevier-Pergamon.

SAUNDERS, A. D., FITTON, J. G., KERR, A. C., NORRY, M. J. & KENT, R. W. 1997. The North Atlantic Igneous Province. In *Large Igneous Provinces: Continental, Oceanic and Planetary Volcanism* (eds J. J. Mahoney & M. F. Coffin), pp. 45–93. American Geophysical Union, Geophysical Monograph no. 100.

SHAW, D. M. 1970. Trace element fractionation during anatexis. *Geochimica et Cosmochimica Acta* **34**, 237–43.

SPANDLER, C., MAVROGENES, J. & HERMANN, J. 2007. Experimental constraints on element mobility from subducted sediments using high-P synthetic fluid/melt inclusions. *Chemical Geology* **239**, 228–49.

SUN, S. S. & MCDONOUGH, W. F. 1989. Chemical and isotopic systematics of oceanic basalts: implications for mantle composition and processes. In *Magmatism in the ocean basins* (eds A. D. Saunders & M. J. Norry), pp. 313–45. Geological Society of London, Special Publication no. 42.

TEPLEY, F. J. & DAVIDSON, J. P. 2003. Mineral-scale Sr-isotope constraints on magma evolution and chamber dynamics in the Rum layered intrusion, Scotland. *Contributions to Mineralogy and Petrology* **145**, 628–41.

THIRLWALL, M. F. & JONES, N. W. 1983. Isotope geochemistry and contamination mechanics of Tertiary lavas from Skye, Northwest Scotland. In *Continental Basalts and Mantle Xenoliths* (eds C. J. Hawkesworth & M. J. Norry), pp. 186–208. Nantwich, Cheshire, UK: Shiva Publishing Limited.

THOMPSON, R. N., DICKIN, A. P., GIBSON, I. L. & MORRISON, M. A. 1982. Elemental fingerprints of isotopic contamination of Hebridean Palaeocene mantle-derived magmas by Archean sial. *Contributions to Mineralogy and Petrology* **79**, 159–68.

THOMPSON, R. N., MORRISON, M. A., DICKIN, A. P., GIBSON, I. L. & HARMON, R. S. 1986. Two contrasting styles of interaction between basic magmas and continental crust in the British Tertiary Volcanic Province. *Journal of Geophysical Research* **91**, 5985–97.

TILLEY, C. E. 1944. A note on the gneisses of Rum. *Geological Magazine* **81**, 129–31.

TROLL, V. R., DONALDSON, C. H. & EMELEUS, C. H. 2004. Pre-eruptive magma mixing in ash-flow deposits in the Tertiary Rum Igneous Centre, Scotland. *Contributions to Mineralogy and Petrology* **147**, 722–39.

TROLL, V. R., EMELEUS, C. H. & DONALDSON, C. H. 2000. Caldera formation in the Rum central igneous complex, Scotland. *Bulletin of Volcanology* **62**, 301–17.

TROLL, V. R., NICOLL, G. R., EMELEUS, C. H. & DONALDSON, C. H. 2008. Dating the onset of volcanism at the Rum Igneous Centre, NW Scotland. *Journal of the Geological Society, London* **165**, 651–9.

UPTON, B. G. J., SKOVGAARD, A. C., MCCLURG, J., KIRSTEIN, L., CHEADLE, M., EMELEUS, C. H., WADWORTH, W. J. & FALLICK, A. E. 2002. Picritic magmas and the Rum ultramafic complex, Scotland. *Geological Magazine* **139**, 437–52.

VIERECK, L. G., HERTOGEN, J., PARSON, L. M., MORTON, A. C., LOVE, D. & GIBSON, I. L. 1989. Chemical stratigraphy and petrology of the Vøring Plateau tholeiitic lavas and interlayered volcaniclastic sediments at ODP Hole 642E. In *Proceedings of the Ocean Drilling Program, Scientific Results, vol. 104* (eds O. Eldholm, J. Thiede, E. Taylor *et al.*), pp. 367–96. College Station, Texas.

VIERECK, L. G., TAYLOR, P. N., PARSON, L. M., MORTON, A. C., HERTOGEN, J. & the ODP Leg 104 Scientific Party. 1988. Origin of the Palaeogene Vøring plateau volcanic sequence. In *Early Tertiary Volcanism and the Opening of the NE Atlantic* (eds A. C. Morton & L. M. Parson), pp. 69–83. Geological Society of London, Special Publication no. 39.

WEAVER, B. L. & TARNEY, J. 1981. Lewisian gneiss geochemistry and Archean crustal development models. *Earth and Planetary Science Letters* **55**, 171–80.

WOOD, D. A. 1980. The application of a Th–Hf–Ta diagram to problems of tectonomagmatic classification and to establishing the nature of crustal contamination of basaltic lavas of the British Tertiary Volcanic Province. *Earth and Planetary Science Letters* **50**, 11–30.

ZACK, T. & JOHN, T. 2007. An evaluation of reactive fluid flow and trace element mobility in subducting slabs. *Chemical Geology* **239**, 199–216.